LARS Contract Report 082478

Synthetic Aperture Radar/Landsat MSS Image Registration System Study

Final Report

by
P. E. Anuta
D. M. Freeman
B. M. Shelley
C. R. Smith

Prepared for
National Aeronautics and Space Administration
Wallops Flight Center
Wallops Island, Virginia 23337

by
The Laboratory for Applications of Remote Sensing
Purdue University
West Lafayette, Indiana 47906

August 1978

STAR (REVERSE OF FORM)

1. Report No. 082478	2. Government Accession No.	3. Recipient's Catalog No
4. Title and Subtitle SYNTHETIC APERTURE RADAR/LANDSAT MSS IMAGE REGISTRATION SYSTEM STUDY - Final Report		5. Report Date 6. Performing Organization Code
7. Author(s) Paul E. Anuta, William M. Shelly, David M. Freeman, Charles R. Smith		8. Performing Organization Report No 082478 10. Work Unit No.
9. Performing Organization Name and Address Purdue University Laboratory for Applications of Remote Sensing (LARS) 1220 Potter Drive, West Lafayette, Indiana 47906		11. Contract or Grant No NAS6-2816 13. Type of Report and Period Covered Final Report
12. Sponsoring Agency Name and Address NASA Wallops Flight Center Wallops Island, Virginia 23337		14. Sponsoring Agency Code
15. Supplementary Notes		

16. Abstract

A study was conducted to determine the algorithms and procedures necessary for registration of imagery from synthetic aperture radar systems and the Landsat multispectral scanner. Three organizations Purdue/LARS, IBM, and Goodyear Aerospace participated. Radiometric and geometric distortions in sample aircraft SAR imagery were analysed and recommendations made for a system to register SAR data to a Landsat reference. This report describes the work done at Purdue under the cited contract. A report including the work done by all three organizations was produced by NASA as a contractor report.

17. Key Words (Suggested by Author(s))	18. Distribution Statement
Landsat Satellite Multispectral Scanners Pattern Registration Radar Imagery Side Looking Radar	

19. Security Classif. (of this report)	20. Security Classif. (of this page)	21. No. of Pages	22. Price*
Unclassified	Unclassified		

*For sale by the National Technical Information Service, Springfield, Virginia 22161

NASA - JSC

TABLE OF CONTENTS

LIST OF FIGURES

LIST OF TABLES

SYNTHETIC APERTURE RADAR/LANDSAT MSS IMAGE REGISTRATION SYSTEM STUDY

I. SUMMARY

The work reported here is the result of a joint study conducted by LARS, IBM Federal Systems Division and Goodyear Aerospace Corporation over the period March 1, 1977 - June 30, 1978 for the NASA Wallops Flight Center. The study addressed the problem of registration of synthetic aperture radar imagery with Landsat multispectral scanner imagery. The interest in combination of these data types arises from the need to improve performance of earth observation information systems over what has been achieved with either type of data alone. A number of methods were tested for registering these data types and the results of these tests are presented. The algorithms, hardware and procedures recommended for implementation in a system for registration of SAR and Landsat data are presented in a system plan. It was the primary intent of the study to define a system which would be resident at LARS and provide services to any qualified user.

II. INTRODUCTION

The study described in this report was initiated in response to a need for an image registration capability for precisely registering Landsat and synthetic aperture radar imagery. Interest is growing in the remote sensing community in the use of imaging radar sensors to augment multispectral scanner data sources in the hope of improving performance over that obtainable from either sensor alone. Current experiments are based on aircraft SAR imagery; however, the SEASAT satellite will provide wide area L band radar imagery over selected land areas. One attractive feature of the radar sensor is its all weather capability

which enables it to provide imagery for missed Landsat overpasses due to cloud cover. Possibly some combination of Landsat and radar imagery over a growing season could provide results not achievable with Landsat alone. Since satellite SAR radar imagery was not available during the course of the study the investigation was based on aircraft SAR imagery.

III. TEST DATA SETS

The study was based on three aircraft SAR data sets which were supplied by NASA Wallops. Time coincident Landsat scenes were obtained for the area covered by the SAR flights. The radar data was flown by the U.S. Air Force using a Goodyear Corp. AN/APQ-102-A X band (nominally 3 cm wavelength) synthetic aperture radar which images a strip nominally 10 N. miles wide. The raw radar data is recorded on film in the form of a phase interference history and further processing is required to produce the imagery. The Environmental Research Institute of Michigan (ERIM) carried out the processing of the raw data film and produced image transparencies of the flight strips. The image film was then scanned and digitized by NASA Wallops using an Optronics P-1700 rotating drum densitometer. The resolution of the processed radar data is in the 10 to 20 meter range and the film digitization was done at 25 meter pixel centers. The film data was recorded in LARSYS byte format and shipped to LARS for the study.

Table 1 lists characteristics of the three data sets considered. The table includes information on the final registered data sets generated by LARS. Control point analysis was carried out on all three sites; but, data was registered only for the second two. The first data set was generated by NASA Wallops in an earlier study. Image reproductions of Data Sets 2 and 3 are presented in Figures 1 through 4.

Table 1. Merged SAR/Landsat Data Set Description. Data stored in LARSYS 3.1 format in tape library at Laboratory for Applications of Remote Sensing, West Lafayette, Indiana.

Data Set No.	Site Identifier	Date of SAR Flight	Landsat Frame/Date	LARS Data Set No.	Number of Lines	No. of Samples/Line	Pixel Size	No. of Channels	Tape No.	File No.
1	Wallops Island, Virginia	August 8, 1973	1403-15125 August 30, 1973	73120104	3352	418	57x79M	6	3352	2
2	Salisbury, Maryland	August 22, 1976	2579-14535 August 23, 1976	76016404	2700	1906	25.4 x 25.4 M	5	3620	1
3	Cambridge, Maryland	August 22, 1976	2579-14535 August 23, 1976	76016413	681	598	25.4 x 25.4 M	7	3692	1

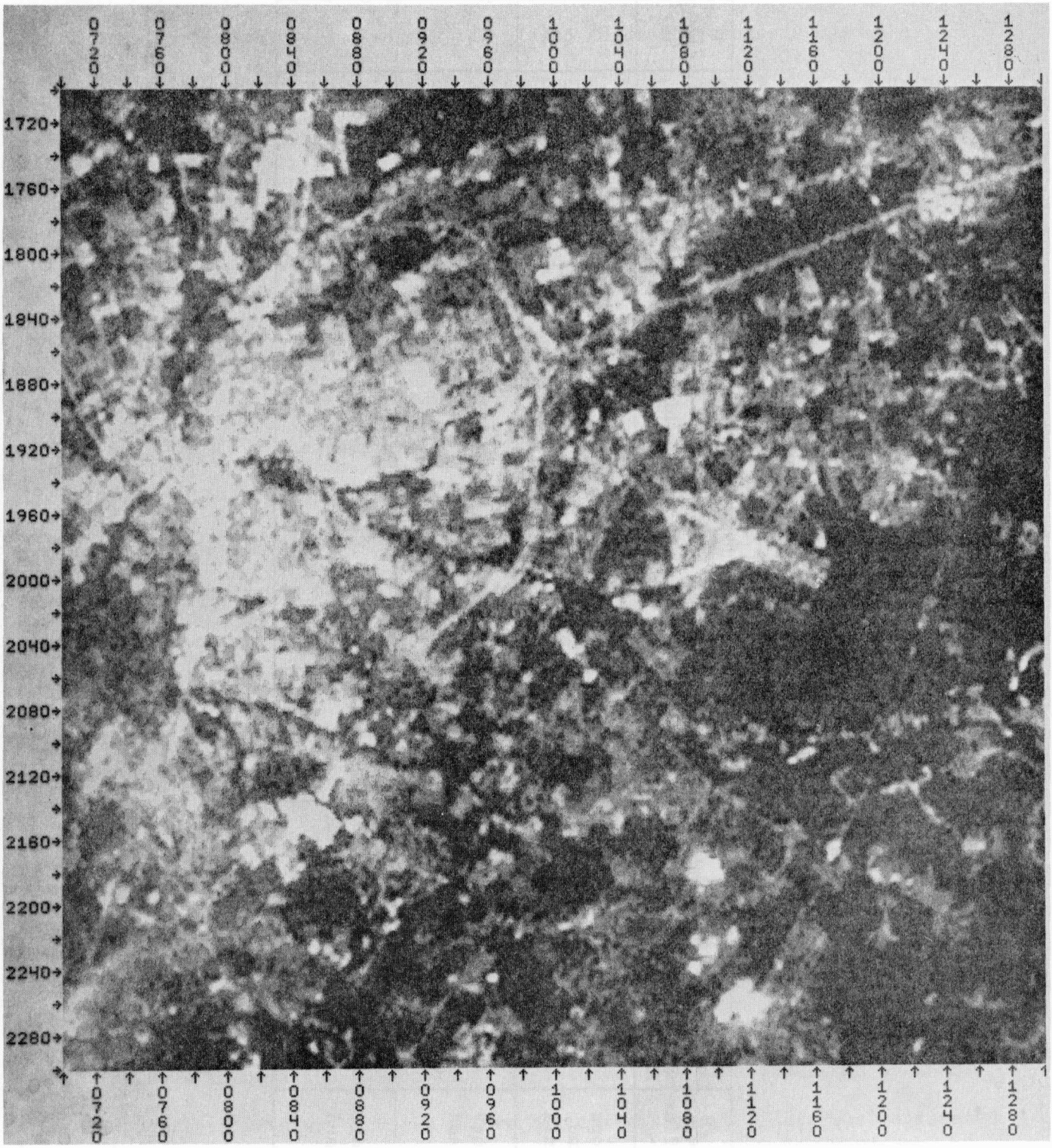

Figure 1. Salisbury, MD. LANDSAT image, channel 2 (0.6-0.7μm), at 25 x 25 meter resolution.

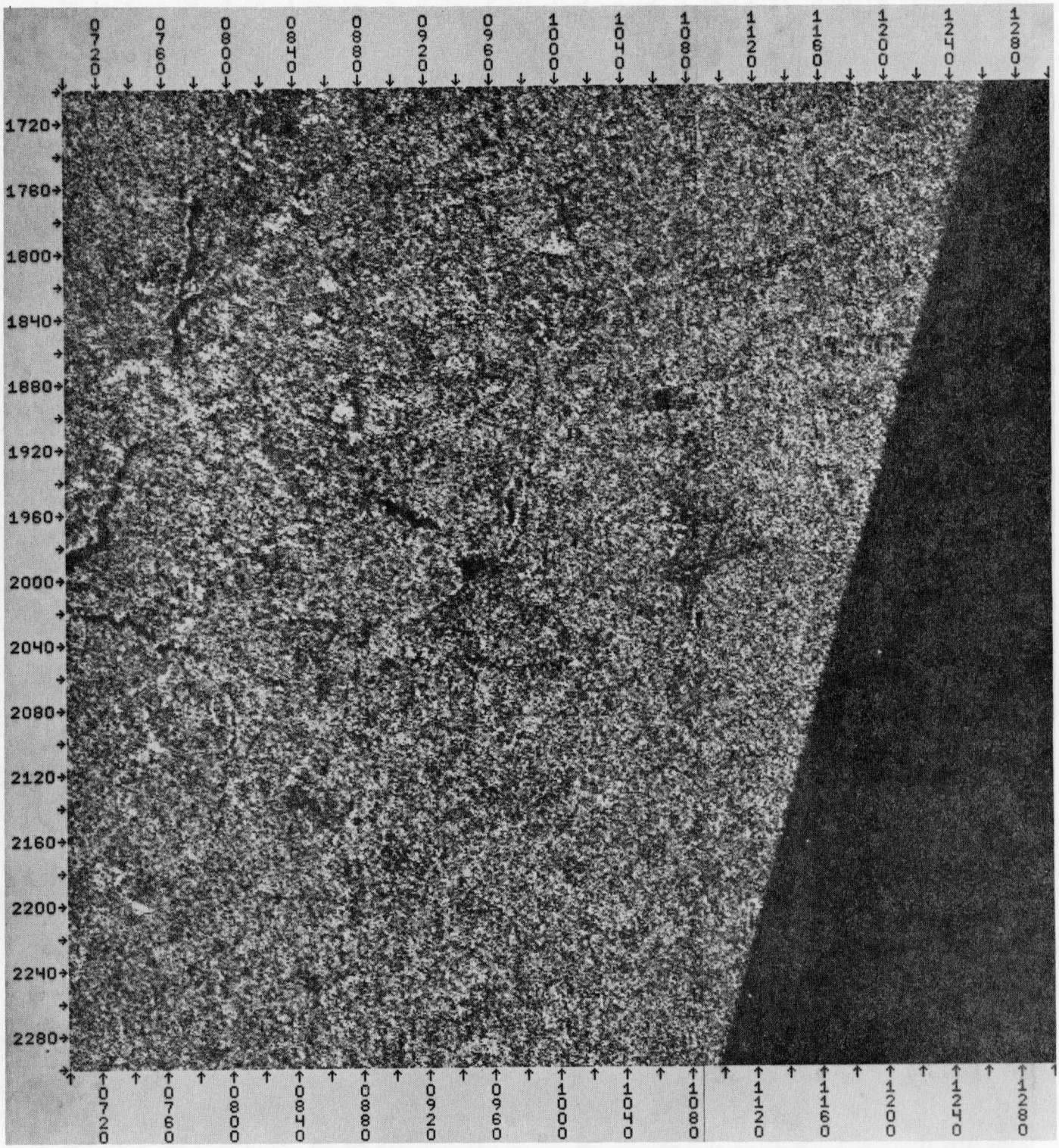

Figure 2. Salisbury, MD. aircraft SAR data registered to 25 x 25 meter resolution LANDSAT.

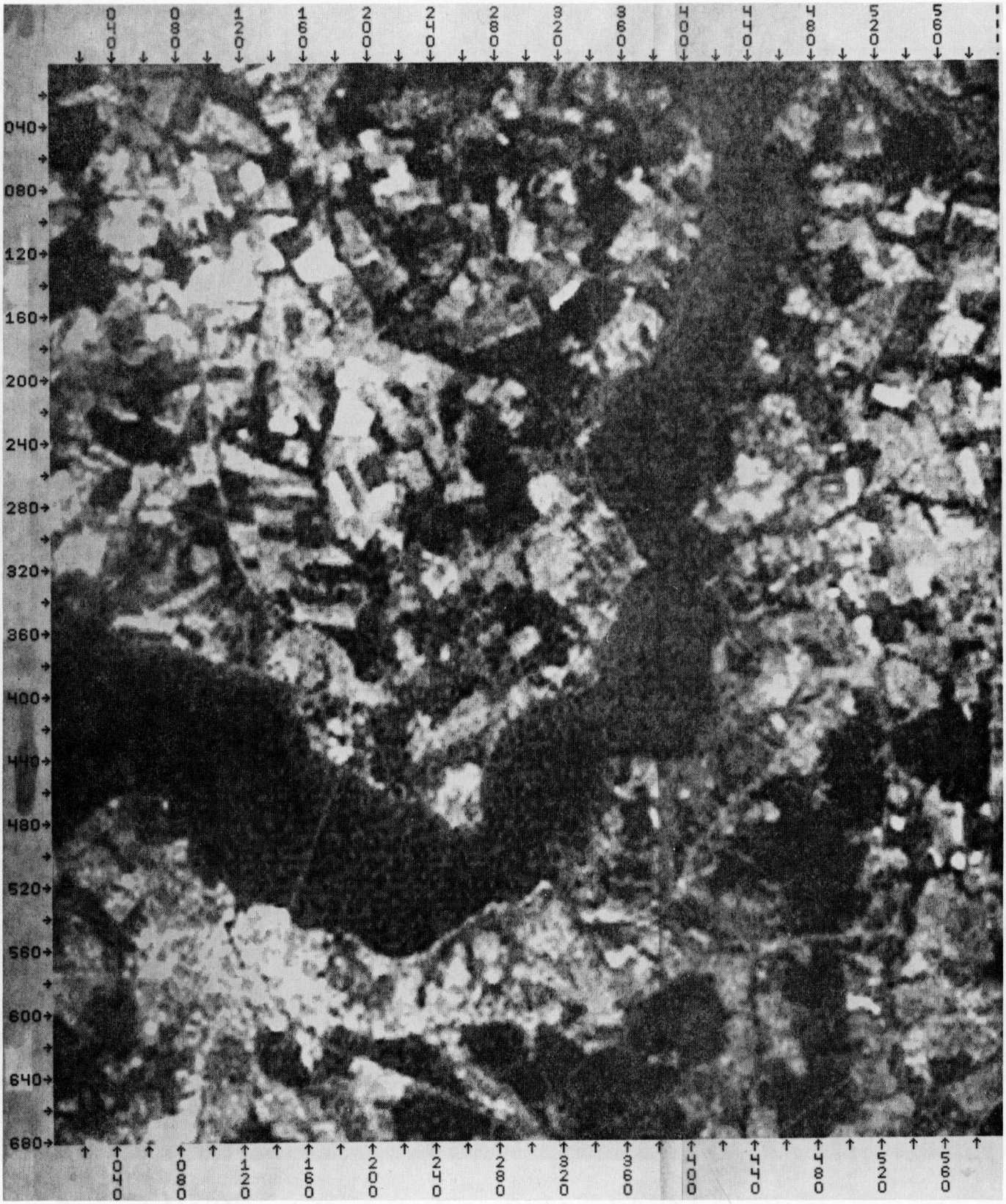

Figure 3. Cambridge, MD, LANDSAT image, channel 2(0.6-0.7μm), at 25 x 25 meter resolution.

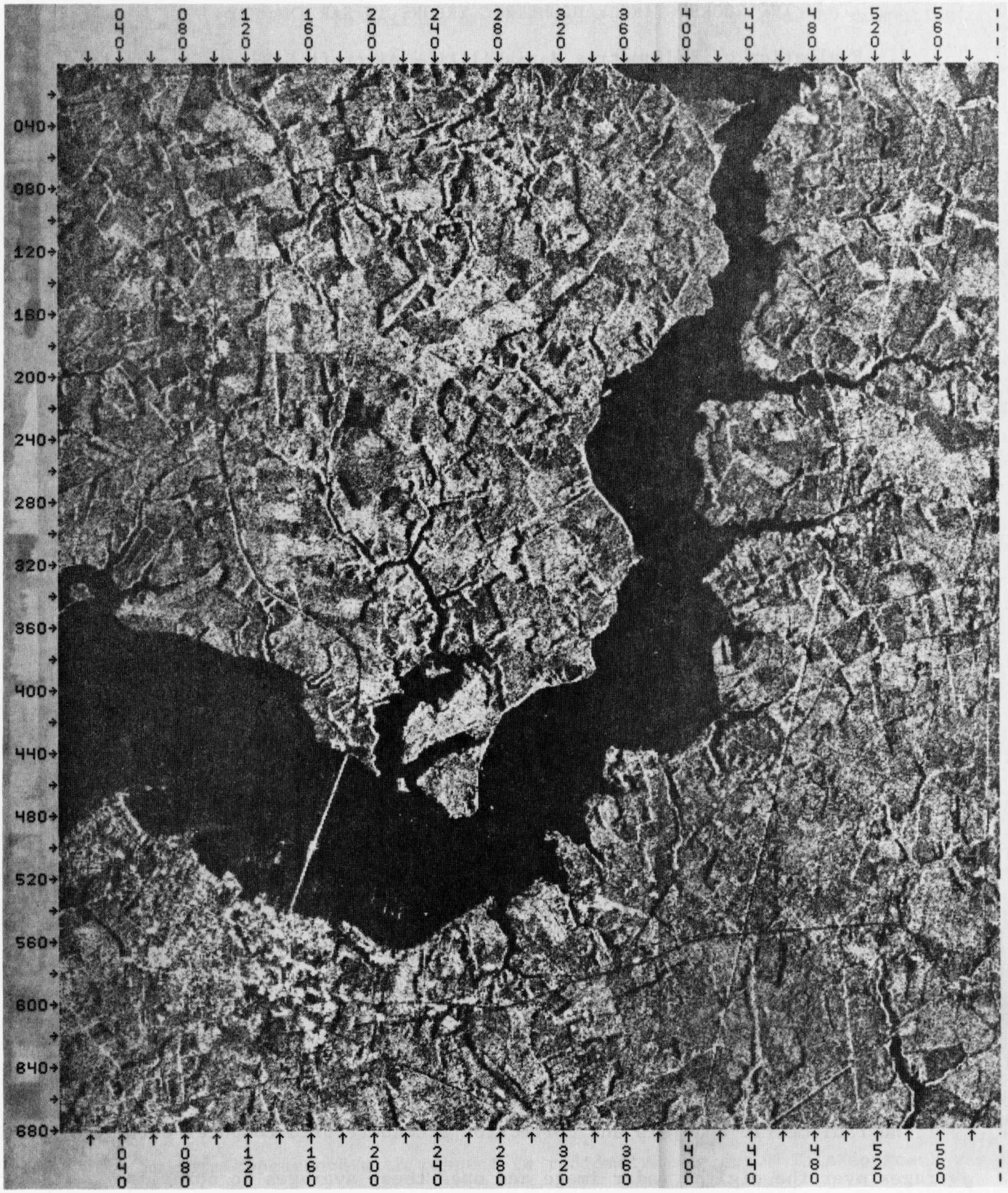

Figure 4. Cambridge, MD. aircraft SAR data registered to 25 x 25 meter LANDSAT.

IV. CORRECTING RADIOMETRIC ERRORS IN SAR IMAGERY

1. Evaluation of Radiometric Variability - Aircraft SAR data can contain radiometric variability due to a number of causes. The primary one is a function of slant range and causes the near image to be brighter than the far image if compensation for this effect is inadequate. Other errors are due to AGC effects, system noise, and film recorder variations both on board the aircraft and in the correlation process. The approach taken in this study was to analyse the resulting image data set for across track and along track variability rather than treat individual error sources separately.

This approach assumes that the radiometric errors are orthogonal in the along track and across track directions and thus can be analysed separately. The digital radar image is stored as an array of numerical values with the columns representing the across track dimension and the lines representing the along track dimension. All the data values in a particular column represent a particular ground range and all values in a line represent a particular along track distance.

Another assumption is made which is scene dependent and must be employed with care; that is that the scene is heterogeneous. This means that the scene classes are distributed uniformly over the area encompassed by the scene so that there are no large areas of one class. This is to say that if the scene contained no radiometric distortions that an average taken over one scene sub-area would be the same as that taken over any other sub-area. The statistical equivalent to this assumption is that the data itself is stationary and any nonstationarity in the scene is the error to be removed.

The radiometric analysis and correction procedure used computes orthogonal averages over the digital radar image and uses these averages to normalize the

data so that the result is uniform or "stationary." This is done by computing an average for each column and for each line in the image as follows:

$$CM_j = \sum_{i=1}^{NLN} x_{ij} \qquad j = 1, NCOL$$

$$LM_i = \sum_{j=1}^{NCOL} x_{ij} \qquad i = 1, NLN$$

where: x_{ij} is the radar image brightness value at column j and line i.

NCOL is the number of columns in the image.

NLN is the number of lines in the image.

CM_j is the column mean for column j.

LM_i is the line mean for line i.

The column and line means are then used to normalize each column and line individually. A standard mean is chosen (SM) and each data value is corrected first across the track and then along track as follows:

$$\hat{Y}_{ij} = \frac{x_{ij}}{CM_j} \times SM \qquad j = 1, NCOL, \quad i = 1, NLN$$

$$Y_{ij} = \frac{\hat{Y}_{ij}}{LM_i} \times SM \qquad i = 1, NLN, \quad j = 1, NCOL$$

where: $\hat{Y}_{ij}$ is the across track corrected radar image value for line i and column j.

Y_{ij} is the line and column corrected image value for line i and column j.

SM is a standard mean value.

A radar image which satisfies the assumptions corrected in this manner will have a uniform appearance with respect to radiometric errors. This approach was tested on the imagery from a SAR flight over Salisbury, Maryland. Figure 5 contains images made from the digital SAR data. The left figure labelled

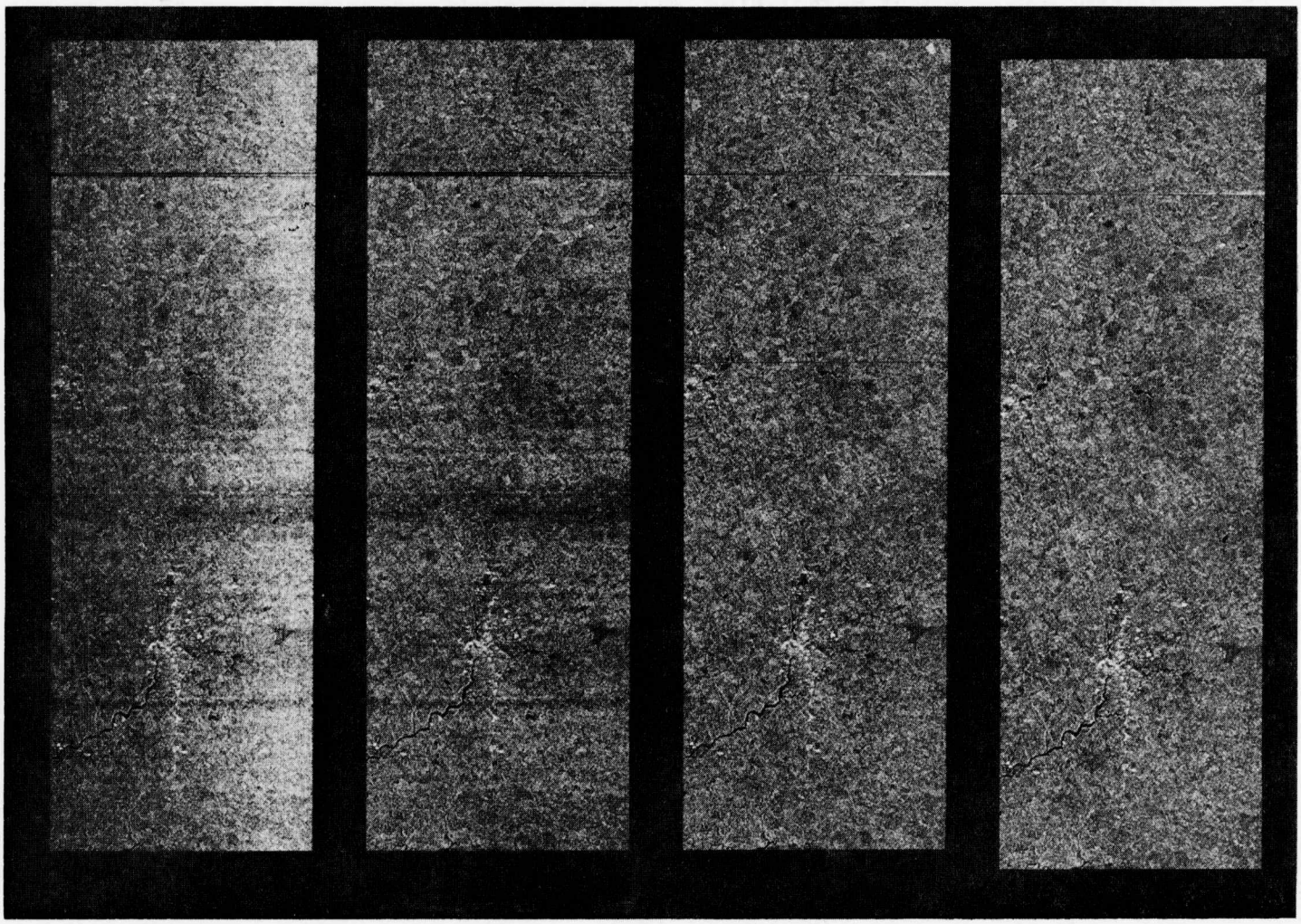

Original | Across Track Corrected | Along Track Corrected | Filtered Data

Figure 5. Radiometric Correction Example Using SAR Data from Salisbury, Maryland.

"original" is seen to contain severe left to right shading which distorts the image and makes it difficult to relate fields on one side of the scene to those on the other side. Other dark bands exist which run along track. In the along track direction several dark bands are seen running across the image and a very dark narrow line exists near the top of the image running across the image. These distortions appear to be orthogonal across and along the image thus satisfying the first assumption. The scene was also judged to be uniformly composed in that there were no large bodies of water or landforms in one area and not in other areas of the scene. The analysis and correction procedure was then applied to the data set.

2. Radiometric Correction Using Line and Column Means - Figure 6 contains a plot of the column averages for the image. The line average graph is essentially flat and was not reproduced here. The general brightness increase from left to right is seen in the column mean graph and the dark bands and very dark line errors can be seen in the line graph plot. The correction procedure for columns produced the second image from the left in Figure 5 and the along track correction applied to the across track corrected scene is presented in the third from left image. It can be seen that the across track shading and along track banding is satisfactorily removed. The correction could, of course, be done in one step but was done separately here to illustrate the effect of each correction. Note that some light shading exists above the right of the very dark error line near the top of the image and a dark area exists near the left end of the line. This is a correction error due to the non-orthogonality of the error; that is, the line is skewed in the image and the averages computed for the lines containing the error do not truly describe the line uniformly from the left to the right of the image. This is an example of the requirement for orthogonality of radiometric errors which must be met for this method.

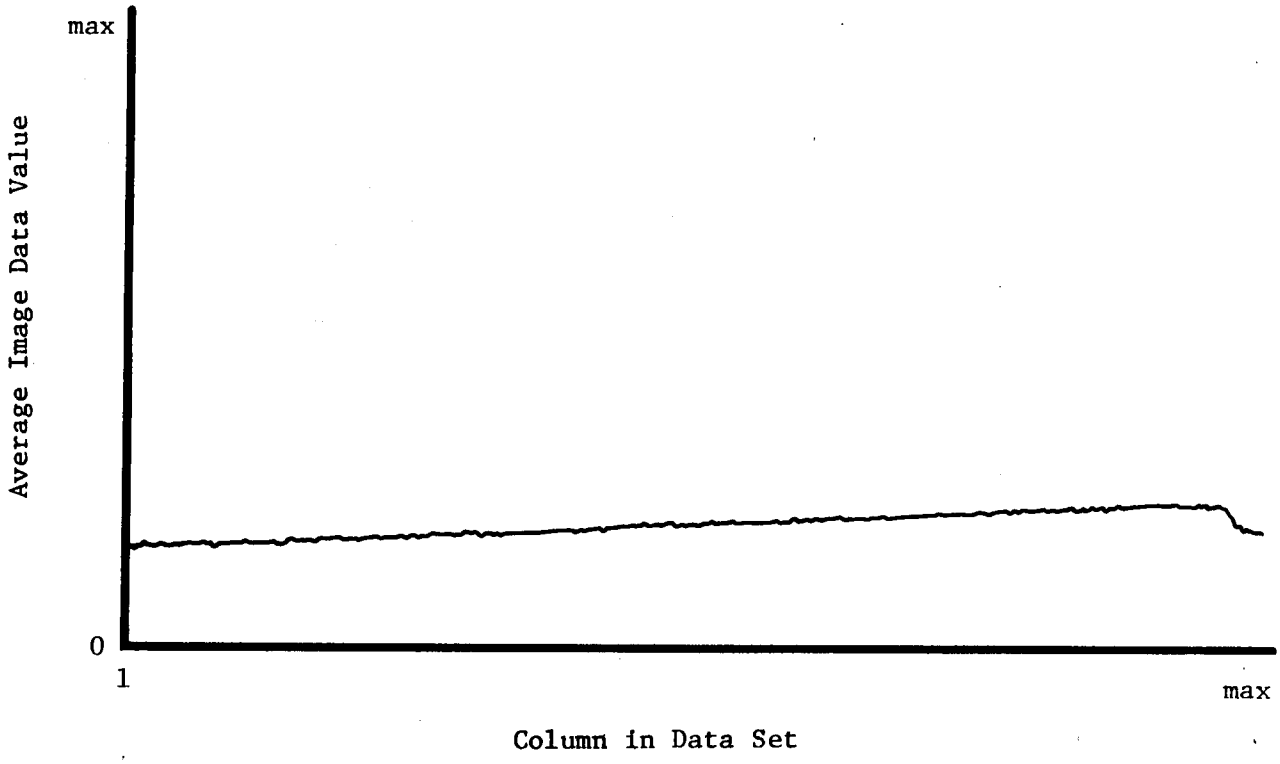

Figure 6. Plot of column means for the Salisbury, Maryland SAR test data. The left side of the image is column one. Note the rise from left to right which corresponds to the increase in brightness in the original image in Figure 5.

The line and column averaging method of correction appears to be a feasible approach for correction of radiometric errors in SAR imagery at least from the aircraft system studied here. Since the method is context based rather than model based it is expected to work equally well on data from other SAR sensors. Model based approaches for the AN/APQ-102A for example would have to compensate for errors in the Sensitivity Time Control and Antenna Illumination pattern compensation. The line-column mean approach will allow users to correct for these and other errors by observing the data rather than fitting a set of models.

3. Two Dimensional Filtering for Noise Reduction - Observation of image reproductions of the Salisbury SAR data revealed a great deal of noisiness which made recognition of scene features difficult. It was decided that some form of image filtering may be desirable in the system if improvement in the signal-to-noise ratio would result. Experimentation was carried out on the Salisbury data to visually observe the effects of filtering.

A sequence of low pass frequency domain filters were tested using a two-dimensional FFT algorithm. Circular filter windows cutting off at frequencies as high as 78% of the Nyquist frequency and as low as 16% were applied to Fourier transforms of subsets of the scene. Figure 7 contains image reproductions of the original and filtered data. The original image is in the upper left position. The subimage is centered on the Salisbury, Maryland airport. The cutoff frequency fractions refer the cutoff frequency to the maximum, or Nyquist, frequency assumed to exist in the image. The subimages used here consisted of a 128 by 128 point block thus the maximum frequency is represented by the 64th point. For example, the 16% or .16 filter passed only the first ten frequencies and set all higher frequencies to zero.

Successive images in Figure 7 represent lower cutoff frequencies and it can be observed that the speckled noise effects become smoother and at the same time the runway in the image blurs out to larger dimensions, both expected

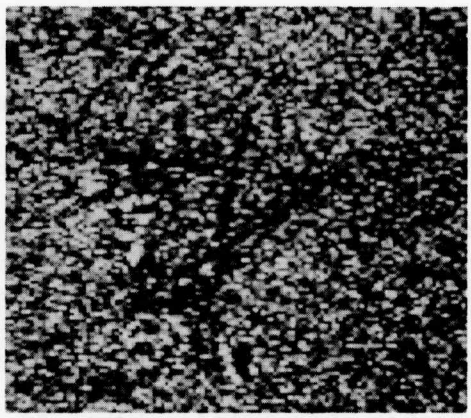

Original Image

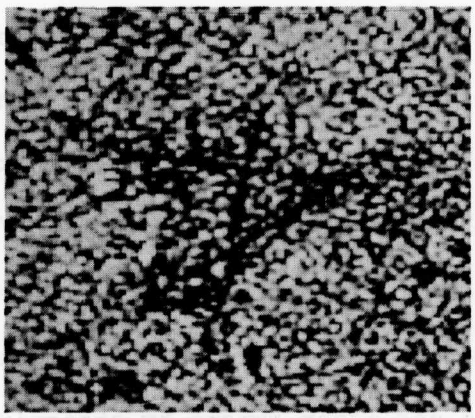

Cutoff Ratio F_c = .78

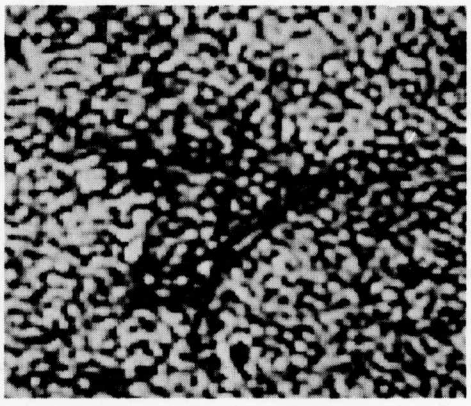

F_c = .63

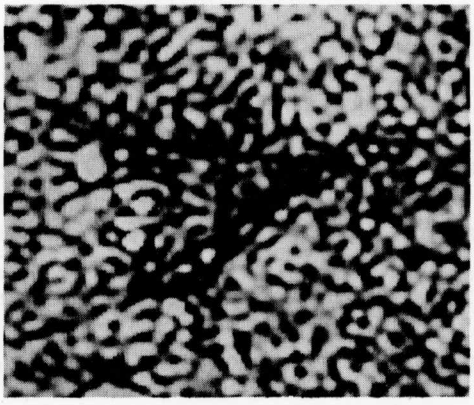

F_c = .47

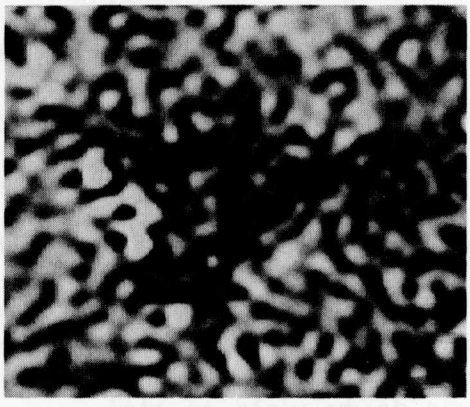

F_c = .31

F_c = .16

Figure 7. Examples of Low Pass Filtered SAR Imagery over Salisbury, Maryland Airport.

results. At the .16 cutoff level the image is seriously blurred and clearly not enough high frequencies are present. On the other hand the .78 cutoff ratio produces very little change in the nature of the image. Visual evaluation suggested that a cutoff somewhere in the .47 to .78 range would smooth the image noise without unacceptably degrading the image.

The FFT filtering approach is cumbersome for larger areas and core limits on the computer used become a limiting factor even at moderate image sizes (e.g., 512 x 512). Thus, a space domain filter must be used to filter the total SAR image and one filter example was thus generated for the Salisbury site. Choice of a filter was dictated by cost considerations as well as image properties. A 2 x 2 equal weight averaging filter has a frequency response with the first minimum at a frequency of 1/2D where D is the sample interval. Power attenuation at the 50% of maximum point is 50% or - 3db at 1/4D. Higher order filters would increase attenuation; however, it was decided that within the cost constraints of the project it would be most useful to run the 2 x 2 averaging filter on the total SAR image as a demonstration. The 2 x 2 filtered image is presented at the right of Figure 5 for the Salisbury site. Slightly greater contrast is observed in the filtered image but the general appearance is not significantly changed. It was decided from this test that filtering would not significantly improve the observers ability to recognize control points in the image. The signal-to-noise ratio of this data is extremely low and filtering evidently does not help this situation. With imagery having better signal-to-noise ratio feature visibility should be better and the need for filtering should be reexamined.

V. CORRECTION OF GEOMETRIC ERRORS IN SAR IMAGERY

Correction of geometric distortions in SAR imagery to achieve registration with a reference required generation of a geometric mapping for each point in

the digital image. The mapping can be based on some systematic model or can use a general polynomial or other functions which are not based on any physical quantity. Both approaches are investigated in this study. A systematic approach developed by Goodyear Aerospace for NASA Wallops was utilized on three test data sets. General polynomials were also employed on the data sets.

The three data sets were all obtained from Air Force flights using the X-Band AN/APQ-102A system over the Delmarva peninsula. These are denoted data sets No. 1, 2, and 3. No. 1 was flown over Wallops Island, Virginia on August 8, 1973. Flights No. 2 and 3 were flown on August 22, 1976 over Salisbury, Maryland (No. 2) and Cambridge, Maryland (No. 3). Data set No. 2 was used in the radiometric correction experiments discussed above. Control points from each of these three data sets were obtained and used in the various models as discussed below. The reference scene used in the case of data sets No. 2. and No. 3 was the geometrically corrected Landsat scene 2579-14535. This data was resampled in a square 25.4 meter grid to a UTM map projection by IBM.

1. Systematic Removal Based on Error Model - The systematic approach was investigated and this section of the report was prepared by NASA Wallops and is included here to enable comparison with the LARS results. This approach is based on an analysis of the geometric distortions to be expected in the SAR imagery. In the systematic approach, the predictable errors are identified and correction terms are generated based on geometric parameters, and so the systematic approach may be useful whenever the geometric distortions can be modeled. The algorithms for removal of these geometric distortions are derived from an understanding of the total radar imaging system from the radar instrument and its aircraft (or spacecraft) platform, through data taking and processing to an interpretable image. The systematic approach is considered here because of its demonstrated usefulness, its simplicity, and its potential

for minimizing computer processing time.

In particular, the images from the AN/APQ-102A used in the examples described in this report exhibit two predictable types of geometric distortion and an orientation problem. The predictable distortions are: skew; and unequal scaling in the along track and cross track directions. Skew (nonorthogonality) of the axes can be caused by radar antenna or correlator slit misalignment. Differential scaling is a result of the separate scaling mechanism involved in the range and track directions. In addition, in general, the digitized SAR image has a grid which has a different orientation than the image or map to which the SAR image is to be registered. If a specific location is to be identified by a common line and column number for all of the registered images, then the two distortions and the orientation problem must be corrected. The imagery of other (not 102A) radar systems would find these algorithms useful if the same type of corrections needed to be applied. This systematic approach does not correct non-linearities in the SAR image that might, for example, be caused by SAR platform perturbations and terrain height variations. If the systematic approach used at Wallops is to be employed to register digitized SAR imagery to a map or to Landsat/map image, then the steps are:

i. The complete SAR image and the corresponding Landsat/map scenes are produced at reduced scale for examination of possible control point locations. The Landsat images examined may include any or all of its spectral bands. A combined Landsat image with its areas classified according to terrain and vegetation may also be used. The control points selected are usually cultural features since they have been found to be more reliable.

ii. Images at full scale of areas surrounding tentative control points are produced for final evaluation. This allows accuracy to the

nearest pixel.

iii. The coordinates of control points from both the SAR image and the Landsat/map image to which the SAR is to be registered are input into the systematic approach algorithm. Outputs of the routine are rotation angle, range scale, track scale and skew angle corrections, along with tables and plots of the residual errors for each control point. The following steps are carried out by the program:

a. The Landsat/map coordinates of the control points are preliminarily aligned with the SAR image coordinates. This is done by determining the relative orientation of two user designated control points in both the SAR image and Landsat/map image frames and then rotating the SAR coordinate system to coincide.

b. A least-squares fit between SAR image and Landsat/map range control point coordinates is performed using the preliminary alignment. The range errors remaining after the fit are computed and the linear correlation coefficient between range errors and track coordinates is determined (if a non-zero coefficient exists, it indicates a residual misalignment). The SAR coordinates are then rotated so as to make the coefficient zero. This process prevents individual control point errors from introducing substantial alignment errors.

c. A least-squares fit between the range coordinates of the SAR image and control point coordinates on the Landsat/map image is computed and residual errors determined (at Landsat/map scale).

d. Track coordinates of the SAR image are scaled to the Landsat/map image via a least-squares fit and average error determined. Skew is then introduced into the SAR coordinate system via two equations:

$Y' = Y$ (1) (X,Y) - original image coordinates

$X'(I) = X(I) + A \cdot Y(I)$ (2) (X',Y') - skewed coordinates

A - tangent of skew angle

The skew angle is varied (in sign and magnitude) until track errors are minimized (as measured by successive least-squares fits).

e. Several types of analyses are then performed by the program in order to demonstrate the relative contribution of various error sources. In each of them, the residual error variance and individual point errors (Landsat/map scale) are computed and displayed for examination after various types of image correction are introduced. The four types of corrections are:

(1) A magnification equal to the average (range and track) scaling difference between SAR and Landsat/map coordinates.

(2) Differential scale correction.

(3) Magnification plus skew correction.

(4) Differential scale and skew correction.

The SAR image range scale, track scale and skew are displayed.

iv. Re-evaluation of the control points takes place using two methods: manual and automatic.

Manual - Most important in this procedure is the final plot produced by the Systematic Approach Program for evaluation by the investigator. It is a layout of the control points in positions corresponding to their relative positions in the image. A vector is attached to each point with the magnitude and direction of its residual error. Its magnitude may be expanded in relation to the scale with which the control points are layed out. If a control point's error vector is unique in magnitude or direction with respect to its neighbors, it is suspected of being inaccurate and it is re-examined in the SAR and Land-

sat/map images. If the vectors in a certain region point in the same direction, this portion may be registered separately for increased accuracy. For example, Data Set #2 was divided into separate sections on this premise. The improvement in results is shown in Table 2.

Table 2. Residual Errors in Reference Frame (RMS) After Registration of Data Set #2 When Using 25.4 Meter Pixels

Section Number	Control Points	Area (km^2)	Residual Errors Along Track (pixels)	Residual Errors Across Track (pixels)
1 of 1	38	1650	10.834	4.692
1 of 2	25	680	5.837	3.664
2 of 2	13	970	5.929	3.828
1 of 4	9	290	1.517	1.272
2 of 4	16	390	5.412	4.394
3 of 4	10	730	2.990	2.663
4 of 4	3	240	.0031	.7334

If magnitudes are large while directions of residual error vectors are without sequence or order, it indicates poor control point selection. In all cases, if the desired accuracy has not been obtained, the control points are re-evaluated and re-input into the program.

Automatic - A modified program may be used which includes automatic control point rejection, in which case it processes the control points and determines if the overall residual error is smaller than an acceptable maximum. If so, it stops; if not, it deletes the control point with the largest error and re-processes the new subset of the original control points. If at the end of the program, a sufficient

number of well distributed control points do not remain, such that all areas of the image cannot be considered adequately registered, manual re-evaluation of the rejected control points is necessary. The program can then be re-run.

2. Polynomial Based Error Removal - Use of first thru fifth degree polynomials was investigated using elements of the Laboratory for Applications of Remote Sensing image registration system and subroutines from standard scientific subroutine packages. IBM FSD also utilized third and fifth order general polynomials to describe the SAR image distortions. The polynomials of degree higher than two were fit to control points from data set No. 2 and No. 3 only. Too few points were available from No. 1 to permit up to fifth degree tests.

The mapping function evaluation carried out was based on the SAR imagery from two flights over the Maryland eastern shore on August 22, 1976. The data set names are "Salisbury" and "Cambridge". Control points were chosen throughout the scenes and conjugate points were located in the Landsat images obtained on August 23, 1976 and geometrically corrected by IBM FSD. The analysis for the two strips will be discussed separately.

A. Salisbury, Maryland SAR Data (Data Set No. 2) - The Salisbury image covered nominally a 16 km (10 mile) wide (across track) by 128 km (80 mile) along track area and 47 control points were chosen over the full width and over a 55 km (34 mile) segment encompassing Salisbury, Maryland. The control points were fitted with two dimensional first through fifth degree polynomials using least square approximation. Large residual errors were observed and certain points were judged as unacceptable and were removed. The fits were recomputed and considerable error remained especially in the along track case. The results of the curve fitting analysis is shown in Table 3.

Table 3. Least Squares Polynomial Approximation Errors for Salisbury Site (Referenced to SAR Grid.)

Type of Polynomial	Section	Along Track RMS Error (Pixels)	Across Track RMS Error (Pixels)	Comments
Affine	Entire	12.5	10.4	Before analysis and deletion of questionable points. (47 initial points).
Affine	Entire	10.4	3.5	After analysis and deletion of points. (34 points remaining).
Affine	Top Half	7.4	2.9	Sections overlap to produce a spline like fit.
Affine	Bottom Half	12.4	3.3	
Biquadratic	Entire	11.9	9.1	Before analysis and deletion of questionable points.
Biquadratic	Entire	9.3	3.2	After analysis and deletion of questionable points.
Biquadratic	Top Fourth	1.4	2.1	
Biquadratic	2nd Fourth	1.6	1.2	Sections overlap to produce a spline like fit.
Biquadratic	3rd Fourth	1.9	1.7	
Biquadratic	Bottom Fourth	1.8	1.5	
Bicubic	Entire	8.7	8.2	Before deletion.
Bicubic	Entire	4.6	2.0	After deletion.
Bicubic	Top Half	2.5	1.6	Sections overlap.
Bicubic	Bottom Half	2.5	1.7	
Biquartic	Entire	7.0	6.9	Before analysis and deletion of bad points.
Biquartic	Entire	3.6	1.8	After deletion.
Biquintic with 3 terms removed		2.5	2.5	34 points used.

The simplest approximation function tested was the Affine model which has the form:

$$v = H_1 + H_2x + H_3y$$

$$u = V_1 + V_2x + V_3y$$

This pair of equations can represent rotation, skew, and scale for the x axis and scale for the y axis. The fit errors for this model are presented first in Table 3. A very large RMS error was observed for the initial 47 points. Each error was inspected and the point was judged valid or misplaced by inspection of the imagery and making and subjective decision. After this process 34 points remained. The fit error was reduced to 10.4 pixels in the along track dimension which was still unacceptably large. The scene was then broken up into along track segments and subsets of the control points used in the model fits. In this case, the smallest along track error observed was 7.4 samples, still an unacceptable error.

A biquadratic model was used next and this equation pair is of the form:

$$v = H_1 + H_2x + H_3y + H_4xy + H_5x^2 + H_6y^2$$

$$u = V_1 + V_2x + V_3y + V_4xy + V_5x^2 + V_6y^2$$

The results for one equation for the entire area were not much better than for the affine case. The site was then divided into four segments and fits made for each segment. In this case, the largest error was 1.9 cells in the along track direction, a reasonable result.

To explore the error characteristics of higher order fits third, fourth, and fifth degree polynomials were fit to the 34 high confidence control points. A standard least squares technique was used to obtain the polynomials. The higher degree cases are conveniently expressed in terms of matrix notation. The fifth degree case will be outlined on the following page. (The fifth degree equations were prepared by IBM FSD.)

Let:

(y_i, x_i) = horizontal and vertical pixel coordinates of i^{th} control point in corrected Landsat space.

(v_i, u_i) = horizontal and vertical pixel coordinates of i^{th} control point in uncorrected SAR space.

$$T = \begin{bmatrix} v_1 & u_1 \\ \vdots & \vdots \\ v_n & u_n \end{bmatrix}$$

$$W = \begin{bmatrix} f_1(y_1,x_1) & \cdots & f_{21}(y_1,x_1) \\ & \vdots & \\ f_1(y_n,x_n) & \cdots & f_{21}(y_n,x_n) \end{bmatrix}$$

$$R = \begin{bmatrix} H_1 & V_1 \\ \vdots & \vdots \\ H_{21} & V_{21} \end{bmatrix}$$

The $f_i(y_j,x_j)$ are the products of powers of x and y.

The columns of R will represent the coefficients of two polynomials. That is,

$$\begin{aligned} H(y,x) = {} & H_1 + H_2x + H_3x^2 + H_4x^3 + H_5x^4 + H_6x^5 + \\ & H_7y + H_8yx + H_9yx^2 + H_{10}yx^3 + H_{11}yx^4 \\ & H_{12}y^2 + H_{13}y^2x + H_{14}y^2x^2 + H_{15}y^2x^3 + \\ & H_{16}y^3 + H_{17}y^3x + H_{18}y^3x^2 + \\ & H_{19}y^4 + H_{20}y^4x + \\ & H_{21}y^5 \end{aligned}$$

$$= \sum_{i=1}^{21} H_i \, f_i(y,x)$$

$$V(y,x) = \sum_{i=1}^{21} V_i f_i(y,x)$$

The polynomials H and V approximate the mapping

$$(y_i,x_i) \longrightarrow (v_i,u_i) \quad \text{for } i=1,2,\ldots,n$$

in the least squares sense. That is,

$$\left.\begin{aligned} H(y_i,x_i) &\approx v_i \\ V(y_i,x_i) &\approx u_i \end{aligned}\right\} \quad \text{for } i = 1,2,\ldots,n$$

The coefficients of H and V are found by solving the matrix equation T=WR for R. The solution is:

$$R = (W^T W)^{-1} W^T T$$

The equations given above are for full, fifth-degree, bivariate polynomials. All other orders use subsets of the terms listed in the above case. In each case, the form of the polynomials was determined empirically. Several polynomials were found by performing the least squares fit, and the resulting residual errors were computed. The ideal situation in doing a direct fit to control points is to have a highly overdetermined system and to have very low residual errors. This would indicate that the polynomials were good models of the geometric distortions. This did not happen for the two images in question.

The bi-cubic polynomial for the entire area produced a large error of 8.7 pixels and when split into two sections the error was still a marginal 2.5. The fourth order polynomial produced a maximum error of 7.0 and the fifth order had an error of 2.5 pixels both over the entire area. Smaller subsets were not used since there are large numbers of terms in the fourth and fifth degree cases and there are only 34 control points.

It was evident from these results that the geometric distortion in the SAR imagery with respect to the rectified Landsat was severe and single polynomials of high order would not represent the distortion adequately. To get a better look at the spatial relationship of the errors the position of each control point was plotted with a vector indicating the fit error and the line and column errors were also plotted in bar graph form along the borders. This plot is shown in Figure 8. The along track (line) error demonstrates an oscillatory nature with at least four peaks over the along track span. The cause of such an oscillation is not known; however, film transport speed variations are a possible cause.

The favorable results using the segmented approach to the polynomial approximation suggested that this was an attractive approach to pursue, since the order of fit in a particular segment is limited. However, it was judged that the nature of the distortions in the Salisbury data set were abnormal and more typical better quality data sets would likely not have such severe distortions. The Cambridge data set (No. 3) proved to be less distorted as is discussed next.

B. Cambridge, Maryland SAR Data (No. 3) - A SAR flight over nearby Cambridge, Maryland produced a data set which was more uniform in geometry than No. 2 and lower curve fit errors were observed. Table 4 contains the RMS errors for affine through fifth order polynomial least square fits to 47 control points. The errors for the biquadratic fit are plotted in Figure 9 with the line and column errors graphed along the edges of the vector plot. The LARS BIQUAD program deletes checkpoints until an error criterion is met.

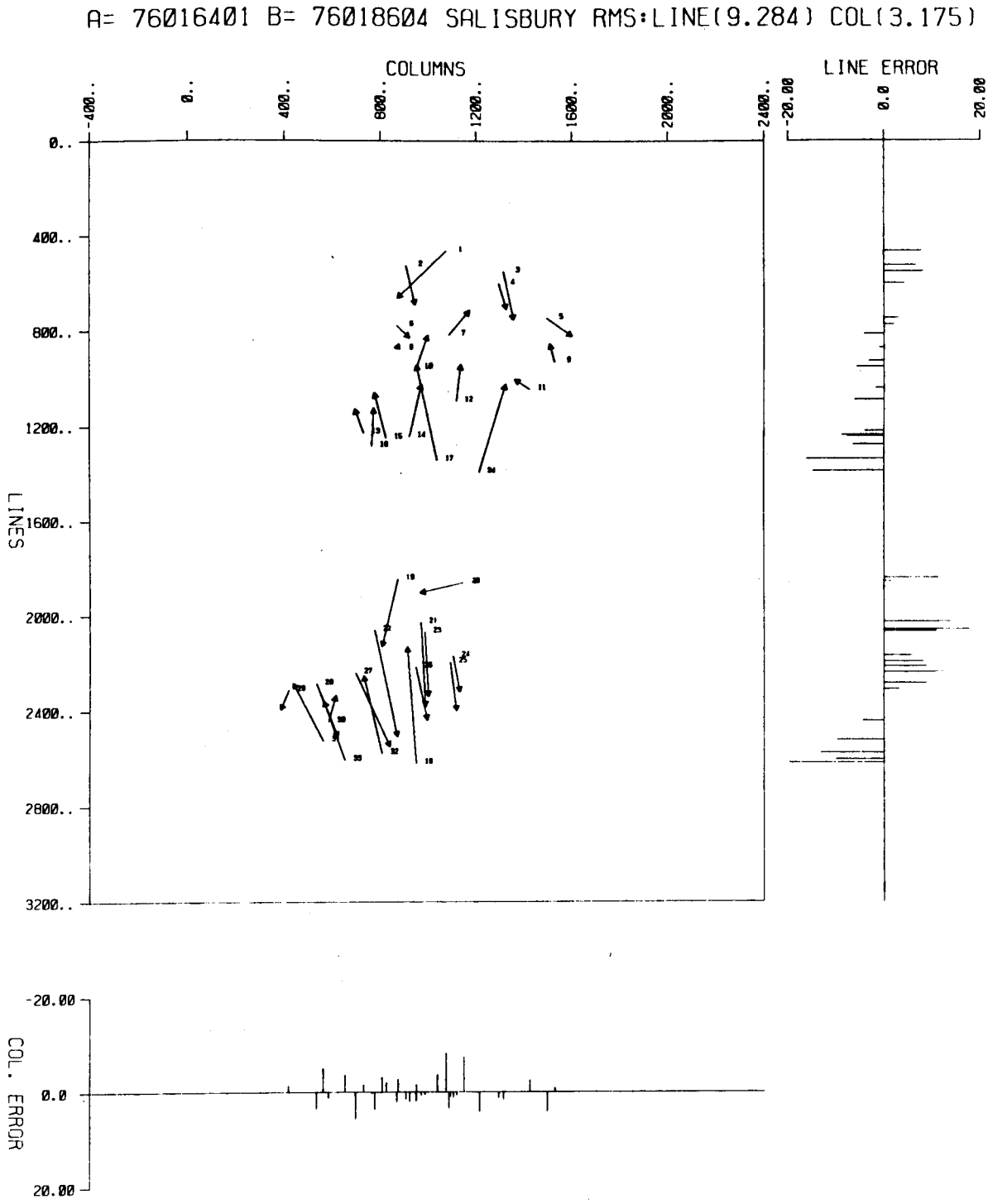

Figure 8. Vector Plot of Residual Control Points Fit Errors for Salisbury Site.

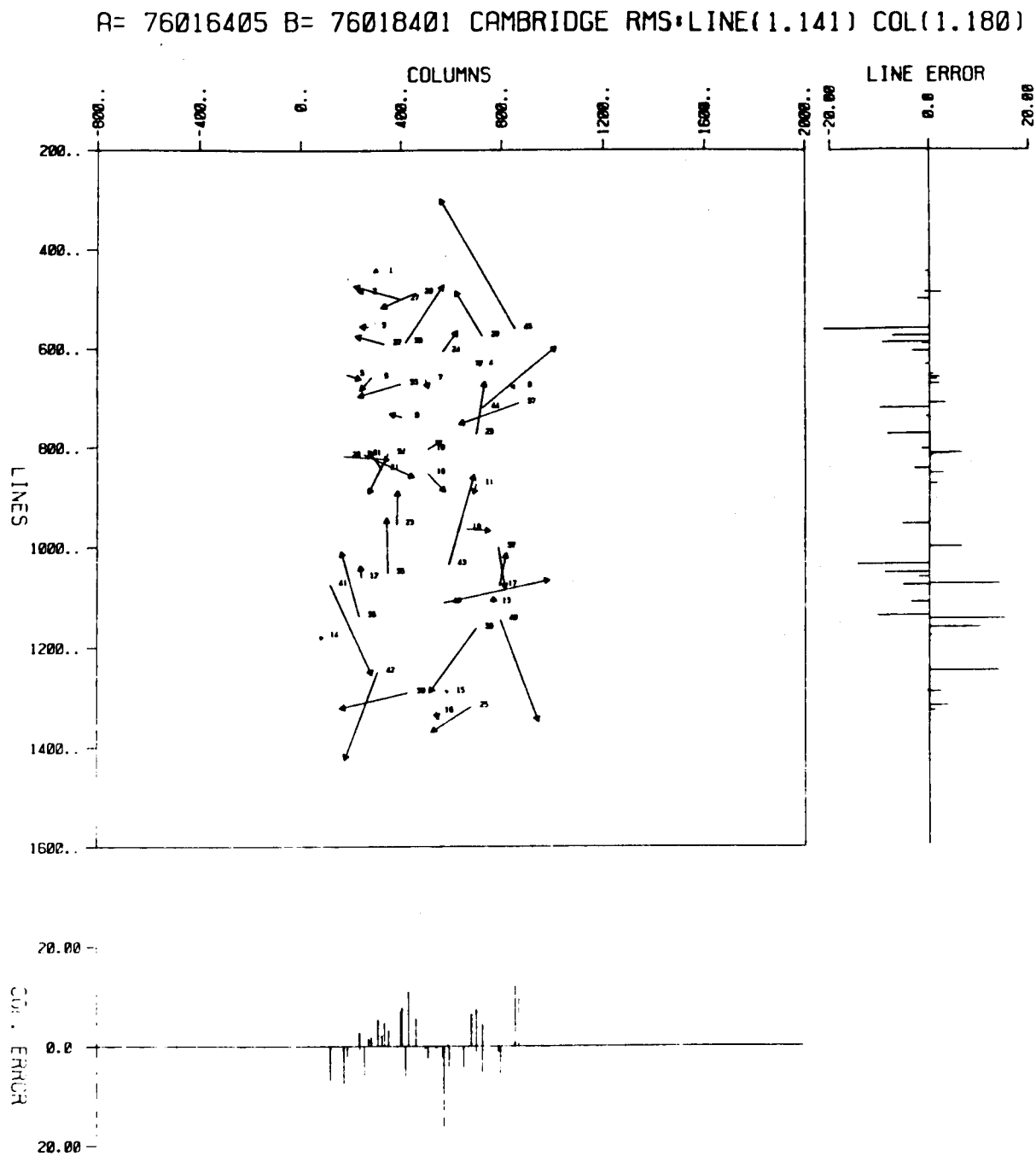

Figure 9. Vector Plot of Control Point Fit Errors for Cambridge Site.

In the case of the Cambridge data, thirty-one points were deleted and the line and column RMS errors quoted are for the sixteen remaining points. All other results in Table 4 are for a fit to 37 points.

Table 4. Residual Errors for Data Set No. 3 (Cambridge) When Using 25.4 Meter Pixels

Registration Approach	RMS Residual Errors Along Track (pixels)	RMS Residual Errors Across Track (pixels)
Systematic*	2.29*	1.83*
Affine	5.00	4.04
Biquad All Points	3.98	3.96
Biquad Reduced Set	1.14	1.18
Second Order Polynomial	4.13	4.16
Third Order Polynomial	4.28	3.48
Fourth Order Polynomial	3.55	3.67
Fifth Order Polynomial	3.82	3.38

*In Landsat reference grid. All other errors in SAR Grid.

Another point should be mentioned, the plots in Figures 8 and 9 are for all the control points considered evaluated by a polynomial fit to the reduced set accepted by the program. In the case of the Cambridge plot, this means that the polynomial was fit to 16 points with a 1.44 and 1.18 line and column RMS error and the error for all 47 points was plotted using this function.

The results of these tests indicate that the systematic and polynomial geometric error modelling approaches provide adequate means of expressing the distortion in good quality small SAR data sets. The performance of the higher

degree polynomials is not significantly better than the quadratic. Furthermore, the cost of actually carrying out a high order polynomial registration on the entire data set would be excessive.

C. Data Set No. 1 Evaluations - The earlier (1973) data set covered a small area and was processed at Landsat resolution (57 x 79 m) rather than 25 m resolution as was Data Set No. 2 and No. 3.

Table 5 contains RMS errors of the pixel differences between control points in the Landsat images and the control points in the SAR images after registration of Data Set No. 1 using the three different approaches. Data Set No. 1 contains 11 control points covering approximately 80 square kilometers.

Table 5. Residual Errors for Data Set No. 1 When Using 79 x 56 Meter Pixels

Registration Approach	RMS Residual Errors Along Track (pixels)	RMS Residual Errors Across Track (pixels)
Systematic	.48*	.49*
Affine	6.53	12.14
Biquad	4.66	8.17

*Systematic Errors in Landsat reference frame.

This result brings out the difficulty of comparing the results of the systematic versus polynomial curve fits. It is shown in the Appendix that the systematic and affine fits are equivalent thus, the two results in Table 5 represent the same error. The systematic errors quoted are with respect to the reference or output grid whereas errors for all the other methods are referenced to the grid of the image to be registered. When the scale factors of the two spaces are the same the results will be the same in either reference which was the case for Data Set No. 2. If the scale factors are

different such as in the case of Data Set No.'s 1 and 3 where the image to be registered (SAR) had a much smaller grid than the reference the systematic error will be different (smaller in this case). Since systematic and affine models are equivalent the errors in the same reference grid would be the same. In Table 5 this means that the biquad result would be lower than affine or systematic in the reference grid and is thus the best result.

Similarly for Data Set No. 3 about a 2 to 1 difference is noted in reference versus SAR grid results (systematic = 2.29 vs. affine = 5.0) thus, the best result is biquad with an approximate .5 pixel error in the reference grid (1.14 divided approximately in half.) The biquadratic result for all points would be around 2 pixels in the reference grid.

Future implementations will express all errors in the reference grid; however, this change could not be implemented in time for use in this study.

VI. CONTROL POINT LOCATION APPROACHES

The basis of registration of Landsat imagery and SAR imagery is the use of conjugate control points found in each image. Registration of Landsat imagery to a geographic coordinate grid is done by manual or automatic control point location. These approaches are discussed separately.

1. Manual

The data sets to be registered must first be reproduced in useful image format. The Landsat image is inspected for scene objects likely to be visible in the SAR image. These can be the control points used to rectify the Landsat image to a geographic coordinate system.

The Landsat control points used may or may not be visible in the SAR image. Thus, the SAR image must be inspected for existence of previously found Landsat control point locations. Once these are exhausted the SAR image is inspected for new points and the corresponding points in the Landsat image

are searched for. Through such a cross inspection process a candidate set of control points is located.

Two factors come into play in the control point selection process. One is the number of points needed and the other is distribution of the points. The minimum number needed is, of course, the number of degrees of freedom (number of coefficients) in the distortion function being used. The advantage in selecting a larger number of points than the minimum is that errors in control point location are averaged and a more accurate fit results. Also, the model will generally not express the true distortions over the image and gathering a larger number of points over the scene averages the errors over the scene.

Distribution of points is important if the distortion function is to be representative of the whole scene. If corners or large regions do not contain control points it is likely that the fit in those areas will be poor.

2. Automatic Control Point Determination

Experimentation was carried out to determine if correlation methods could be used to define control points for registration of SAR and Landsat. In an operational situation the correlation would be done between original Landsat and SAR imagery which were different in rotation and other distortions. The numerical correlation process requires that the two images being correlated have the same rotational alignment and scale. This can be accomplished by performing a preliminary affine correction to one of the images before correlation. The correlator would then be employed to find small residual translational errors remaining.

A numerical correlation processor was applied to the Salisbury and Cambridge data sets to explore the correlation potential of SAR and Landsat imagery. The correlations observed in a large number of tests were all very low (less than 50% correlation) and the tests were judged to be negative for these two cases.

Further experimentation was beyond the scope of the present study; however, higher contrast SAR imagery and appropriate enhancement of the SAR and Landsat images may produce useful automatic correlation results. Thus, automatic control point finding in SAR/Landsat scene pairs is recommended for future study.

VII. RESAMPLING CONSIDERATIONS FOR SAR

Whenever registration of two or more digital image data sets which were sampled at different rates and over different grids is attempted the problem of resampling arises. This results since no samples exist at corresponding points in the scene for each image to be registered. A number of resampling schemes exist which are widely used in the image processing field. The simplest of these is called nearest neighbor (NN) resampling and is implemented by assigning the value of the nearest pixel to the location being resampled. Higher order resampling is the term applied to the use of linear, quadratic cubic and higher order polynomials in the resampling process. More advanced interpolation and filtering techniques can also be used which in some sense optimally filters the unwanted frequencies and resamples the image with minimum loss of the desired frequencies.

In the case of SAR registration considered here, the sampling grid for the radar data was nominally 25 meters. The Landsat data to which the SAR data is to be registered is sampled at 57 meters in the across track direction and 79 meters in the along track direction. The Landsat data thus must be resampled to 25 meters to match the SAR data. In the registration process the SAR data is geometrically transformed; but, since the "before" and "after" grids are both 25 meters no scale change is necessary. Thus, the problem of resampling the Landsat data was studied and the assumption that nearest neighbor resampling would be adequate for the SAR data was made. The maximum position error for square grid nearest neighbor resampling is $D/\sqrt{2}$ or for this case $25/\sqrt{2} = 17.7$ meters. For the

Landsat data the NN error would be much larger and the project resources were thus put into the Landsat resampling problem which was studied by IBM FSD. Further study is needed of the effects of higher order resampling on the SAR image.

VIII. SUMMARY OF SAR INVESTIGATION

The investigation of SAR radiometric and geometric characteristics discussed above was a very limited look at the SAR/Landsat merging problem. Only three data sets were studied and of these one was of good radiometric and geometric quality. Due to LARS inexperience with SAR data and the unexpectedly poor geometric and image quality of the Salisbury data set which, was intended as the main data set for the study, most of the resources were expended in data handling, imaging and unproductive registration experiments. Nonetheless, significant insight into the SAR registration problem obtained. The major elements of the process are spectral correction, spatial correction and control point determination.

The spectral characteristics of SAR are markedly different than Landsat or other optical reflective data. In addition to very long wavelengths relative to the optical, the look angles are large and dynamic ranges are extreme. The result is imagery that is difficult to relate to a Landsat reference. The main purpose of the study was to establish registration requirements and although initially discussed data useage was not included as a final requirement. Spectral characteristics were considered as an aid in the registration process and two processes were investigated. Both along and across track normalization were tested as was low pass filtering. These were determined to be useful cosmetic processes, but their value for aiding registration was questionable. The effect on classification performance was not tested; but, it was intuitively believed that better along track and

across track uniformity of the image would result in higher quality of analysis. Based on these results, it was decided that the SAR registration system should include the optional capability to perform along and across track shading corrections and to low pass filter the image.

Spatial considerations were based on visually determined control points in three SAR/Landsat data sets. Spatial distortions in one of the data sets was severe enough to prevent modeling to sub-pixel accuracy by first through fifth degree polynomials. Image production problems were suspected as being the cause of large distortions in this data set (No. 2) and results for this case are not considered typical. The problem of finding additional control points and computational problems in using high degree polynomials limited the investigation to fifth degree and there are problems even at fifth degree. In data set No. 3, biquadratic results were sub-pixel for a reduced set of points; but, for all points the error was around 2 reference pixels. Higher degree fits were not significantly better. For data set No. 3 a linear fit achieved sub-pixel accuracy. Thus, it is not clear from the study what degree of fit is needed; however, significant insight was obtained. It is recommended that up to fifth degree capability be provided in a final system with up to third degree provided in near term implementations.

Control point finding procedures were investigated and automatic (correlation) methods did not work in the tests carried out. Thus, manual (visual) methods are recommended for initial systems. The imagery problem is significant for this process and a combination of small format high resolution film writer output and large format graphics printer output is recommended for user control point finding. The high resolution film product is useful for large area feature recognition and the large format output is necessary for precise control point coordinate determination.

IX. SAR/LANDSAT DATA MERGING SYSTEM STRUCTURE

A. Introduction

The SAR/Landsat data merging system is required to provide the remote sensing community with a capability to access for analysis and further research registered data from these two sensor systems. While general registration procedures apply, special considerations must be made to cover this multisensor application. The considerations are quite broad, based on the fact that the radar data comes from multiple sources such as aircraft and satellites. In contrast Landsat data is a relatively stabilized input data source with better known parameters. This discussion indicates that a solid generalized design SAR/Landsat data merging system is required to assure the remote sensing community access to this multisensor data.

Elements of the study of the SAR/Landsat data merging system include functional, hardware and software requirements. In addition, special user considerations and a suggested implementation plan are presented. A few comments will be made to establish a background for each of these topics.

Functional requirements refer to the basic conceptual actions which may be performed using the system of programs which make up the SAR/Landsat data merging system. Data sources and parameters are defined and input reformatting programs provided.

The reformatted input data must be imaged, and radiometric as well as geometric enhancements applied as needed. Data magnification by changing pixel spacing as well as data orientation to a true north-south grid are examples. Both SAR and Landsat data share these functional requirements.

Programs with algorithms for the actual registration of the data will be included. These programs include the ability to model geometric errors. Control point acquirement is a problem to be addressed. Various interpolation schemes may be utilized.

Finally, intermixed with these is the requirement for imaging. Imaging is critical in virtually all stages of the registration process. Data display needs vary from the basic line printer, to matrix line printing, to digital film writing at high resolutions.

In summary, the functional requirements cover the data merging systems input processing, registration, and output processes. Hardware and software are significantly impacted by these functional requirements.

Hardware specifications and requirements must coordinate with the functional requirements. The size and complexity of the data sets make a large main frame computer with virtual memory addressing desirable. Programs and programmers become less hindered by computer memory space constraints when a large main frame with virtual memory is available. Developments tend to progress faster. Magnetic tape will be the primary image data storage medium. Instructions of the computer might be enhanced by an array processor. The number of data sets which may be processed will be influenced by the flexibility and power of the computing equipment. Special hardcopy imaging hardware should also be considered as part of a total system requirement.

Software implements the functional requirements in coordination with hardware. An operating system which supports relatively unlimited address or program space, is important. Restart capability for programs is important so that long execution times are not threatened by intermittent system failure. More powerful efficient compilers will ensure that program execution will be as fast as possible. Careful choice of software implementation will be needed to ensure maximum use of hardware strengths with minimum of functional constraints.

B. FUNCTIONAL REQUIREMENTS

The SAR/Landsat data merging system will have the capability of producing SAR and Landsat MSS images that are registered to each other and to a Universal Transverse Mercator (UTM) map projection. A system user will accomplish this by processing the Landsat data to his own specifications and then processing the SAR data to register with the corrected Landsat data. He can then use the corrected SAR and Landsat data for multispectral classification and other information extraction processes.

There are four major functional requirements for the SAR/Landsat data merging system. First, is the need for data. Second, is a system of inputting that data for use on a system prior to registration. Third, is registration of the data. And lastly, the display of the data throughout the processes of input, registration, and final output states is required.

Data Sources

The sources of SAR and Landsat data are proposed to be the SEASAT and Landsat satellite, respectively. However, some SAR data may also be acquired from other sources as aircraft sensing systems. Landsat data may be acquired from any of three similar Landsat satellites launched between 1972 and 1978. SAR data are not always available immediately in digital format. The capabilities to form an image from a SAR analog data tape as well as digitize the resulting image are necessary. Input may then be made to the reformatting software. Normally radar image formation will be accomplished by highly specialized equipment. The process is known as correlation of the radar data. The user is expected to furnish correlated digital SAR image data.

Data Input

The function of data input is composed of two processes. The first process is the reformatting of the data to a common or standard image format. At LARS

this format is known as LARSYS format. Both Landsat and SAR data may be transformed into this format.

The second process is data enhancement. This represents the preparation necessary for further processing and registration of the data from the Landsat and radar systems. Enhancement may be broken down into cosmetics, radiometric and geometric classes. These classes overlap and complement each other. For instance, a cosmetic fix of a bad line may have special radiometric considerations. Radiometric considerations are part of any magnification method applied to the data. As well, radiometric parameters are a part of any geometric enhancement. An example is the transformation of the Landsat data to some specified grid with true north orientation. Pixel spacing or resolution is an integral part of these processes as well. Algorithms must be available for all three of these functions to aid high quality image formation, as well as control pointing and location or grid definition.

The specific Landsat processing functions that the system will have are:

1. Radiometric correction
2. Geometric correction

Radiometric correction is defined to be a striping reduction process that is performed on MSS data that has been radiometrically calibrated, but not resampled. Geometric correction is defined to be the resampling of MSS data to a UTM map projection. The user will be able to specify both the spacing between pixels in the output UTM image and the orientation of the image (i.e., the direction of north relative to the image scan lines).

The SAR processing functions fall into the same two categories, but different operations are performed. Specific radiometric correction processes that will be available for SAR are shading removal and spatial filtering to reduce speckle, and a generalized polynomial distortion representation for geometric correction will be included.

Data Registration

The registration processing for SAR/Landsat imagery has several requirements. These include numerous image enhancements, a manual control pointing function, an error modeling function and a registration process with various powers of transformation for location matching as well as radiometric interpolation.

Image enhancements may be furnished by the data input phase. Among the enhancements needed will be various filters to smooth data response from side to side as well as top to bottom of a data set.

Control pointing the images from the two scanner systems is accomplished manually. Manual control pointing requires an excellent imaging capability which will be discussed further under the topic of data output products.

Actual data registration will depend on the error modeling. The control points are input to these error modeling programs. Transformations of various powers should be available as outputs. Data registration follows this step.

Data registration should output a registered data set which transforms one or both of the scanner images into a common grid with the other. This grid may be a reference standard different from either of the input scanner data grids. In contrast, one of the two scanner grids may be previously selected as the reference standard and the other scanner data subsequently registered to the same. Further, the reference standard may be a map to which one or both data sets have been registered.

Data Output

Output products are a necessary complement to SAR/Landsat merging system. The output function may take any of several forms. Permanent or semi-permanent imaging is needed to preview data. The same is true to observe intermediate results. Acquiring checkpoints is a function performed at the intermediate

stage. Outputs are equally required to show the comparison. Images may be displayed giving the before and after transformation comparison. Graphics may be used to show final error reduction residue achieved.

Data output capabilities should cover the spectrum from character to matrix gray level to false color photographic. Furthermore, the outputs should be from inexpensive work copies to more expensive digital black and white photographs to fine quality digital color maps. Complimenting any of these may be a temporary image displayed by a CRT device.

Data output represents the tangible glue which constantly compliments the various levels of the data merging system. Each level may have specific demands which some form of data display may answer. The results of the merging system may be transmitted to the user in a significant way through the use of selectively chosen quality data output products. Thus, filmwriting as well as printer plotter and CRT outputs will be vitally important to the success of the data merging system.

C. Hardware Requirements

The SAR/Landsat merging system will be implemented on the IBM 370/148 computer at the Laboratory for Applications of Remote Sensing (LARS) at Purdue University. The only hardware requirements for the system are the tape drives needed for image data sets and sufficient virtual memory for the resampling program. The system will be designed to minimize the use of disk space by using tapes wherever it is reasonable to do so.

The resampling program will require an internal input buffer large enough to store the maximum number of input image lines that will be needed to create one output image line. This is a function of the rotational difference between the input and output images. Therefore, the memory requirements vary from image to image.

D. Software Requirements

The system will be written in Fortran IV and IBM370 Assembler Language. Generally, Fortran will be used wherever it is reasonable to do so. However, Assembler Language Fortran will be used for those programs that would be significantly more inefficient if written in Fortran.

The programs will use some local LARS programs to perform certain standard functions. For example, the program TAPOP will be used to perform image data set I/O.

E. User Considerations

Users of the SAR/Landsat data merging system have several choices to make when processing a Landsat data set. These user options are discussed in this section.

In some cases, a user will have a choice of using partially processed or fully corrected input MSS data. Since fully corrected data are already resampled to a standard map projection, further resampling may not be necessary. A common reason for further resampling would be the need to have the corrected Landsat data at a different pixel spacing than the 57 meters (horizontal and vertical) of the fully corrected data set. Although resampling the data only once is clearly desirable, a recent study (Bi-resampled Data Study; Final Report for Contract NAS5-23708; R. Benner, W. Young; IBM Corp., March 1977) has indicated that a second resampling will degrade the data only slightly and will not essentially change multispectral classification results.

When processing uncorrected MSS data and some partially processed MSS data, a merging system user must decide whether to use geodetic control points in determining the geometric transformation between the corrected and uncorrected spaces. If a systematic correction will provide satisfactory geometric accuracy to meet a user's needs and if no control-point library

exists for a particular scene, then the expense of control-point location can be avoided by using systematic correction.

The system will have the capability to resample with nearest neighbor or cubic convolution. Although cubic convolution is widely regarded as a better algorithm than nearest neighbor, it is considerably more expensive to perform on a general purpose computer. Potential resampling algorithms for the merging system are summaried in Table 6. Computer expense for resampling is directly proportional to the number of pixels that are being created. CPU estimates for the direct algorithms are extrapolations based on running times for an experimental prototype program on an IBM 370/168 Model 3 computer. Estimates for the hybrid-space algorithms are further extrapolations from the direct-program results.

Table 6. Estimated IBM 370/148 CPU Time for Resampling

(Prepared by IBM FSD)

Description of Resampling Algorithm	CPU Minutes per Million Output Pixels
Nearest Neighbor (Direct)	1.7
Cubic Convolution (Direct)	7.7
Cubic Convolution (Direct) with approximate high-frequency MSS correction	11.5
Cubic Convolution (Direct) with exact high-frequency MSS correction	15.0
Cubic Convolution (Hybrid Space)	(3.9)
Cubic Convolution (Hybrid space) with exact high-frequency MSS correction	(5.0)

Pixel spacing in the corrected Landsat data is a user option in the system. MSS input data are spaced at about 57 meters horizontally and at about 79 meters vertically. Fully corrected MSS data produced by the Master Data Processor at NASA Goddard will be spaced at 57 meters in both directions. The spacing in the images processed during the experiments (described in a previous section) was 25.4 meters. This particular spacing was chosen because the SAR data had a similar spacing. A second factor that a user must consider when choosing the pixel spacing is resampling cost. The number of output pixels that are created in the resampling step is inversely proportional to the pixel spacing.

Another user option for Landsat MSS processing is the orientation of the image. Orientation is the angle between north and an image scan line at some point in the image. The standard orientation is such that the spacecraft velocity vector is approximately perpendicular to the image scan lines. That is, input-space scan lines are nearly parallel to output-space scan lines. Orientation affects the resampling step. The memory required for the resampling program is directly proportional to the angle between the input-space scan lines and the output-space scan lines.

Many of the user considerations for the SAR data will be similar to those for processing Landsat data. The user will have several options during the processing of his data.

The first will be cosmetic in nature for bad data lines, i.e., a special case of radiometric correction. The primary method available will be repetition of the immediately preceding good data line. Other algorithms may be programmed at user request and expense.

Second, radiometric corrections will be available in terms of shading corrections along/across track as well as a low pass speckle removing filter.

The use of none or all of these is up to the user. At the present time, they are recommended as a package for the current aircraft SAR imagery.

Third, registration between the SAR and corrected Landsat data may be done via several polynomial functions. An evaluation of these functions will help the user determine whether a linear, biquadratic, cubic or potentially higher degree fit is required. Initially, the choices will be linear and biquadratic. Higher degree functions are planned for future phases of the project. Cost of registration is directly proportional to the complexity of the polynomial used.

Fourth, the resampling of SAR data to the corrected Landsat data grid has similar implications to the Landsat resampling discussion. Essentially, use of the nearest neighbor interpolation will be considerably less expensive than the more image enhancing cubic interpolation.

Fifth, imaging of SAR or Landsat data may be done in several ways as lineprinter, graylevel, printer plotter, CRT and filmwriter. While acquiring control points, however, the highest quality images are required. Generally, filmwriter output is best. It is important to request promptly such outputs very early in the process as special reformatting and outside vendors must be contacted and coordinated to produce the outputs. Size and enhancements must be completed before permanent or semi-permanent filmwriter outputs are attempted. When resident filmwriting is available, turnaround and coordination will be reduced.

F. LARS Implementation Approach

The Landsat/SAR data merging system will be implemented at LARS so that the user community may bring their corresponding Landsat data and SAR data, and obtain a set of registered multisensor image data. Users will assist in the registration process to a degree of their choosing and especially during checkpoint acquirement and data verification.

Implementation of this system (see Figure 10) is expected to be a multi-stage (year) project. In the first of three stages, the most critical portion of the SAR Landsat merging system will be implemented. Reformatting, geometric correction, and selected filtering of Landsat data is included. SAR data reformatting as well as selected basic filtering will be implemented. Limited imaging facilities present in this stage are to be augmented during later stages. Manual checkpoint acquirement is to be utilized. Distortion function evaluation made available during the first stage will include that for systematic, affine, biquadratic and bicubic. The most important part of the system, registration, will be available to provide up to third degree registration and resampling to include nearest neighbor and cubic interpolation. Phase I will provide solid foundation with all essential requirements of the SAR/Landsat data merging system.

Specific tasks for Phase I will be broken down by processing levels. These processing levels include reformatting, geometric correction, filtering, imaging, checkpointing, distortion evaluation, registration and resampling. The proposed system is diagrammed in Figure 10 and the following approach sections will discuss blocks or groups of blocks in this figure.

1. Input Data Reformatting

Reformatting of the Landsat data will be handled by the IBM software. Verification of this software will be a task at this level. SAR data reformatting programs exist and will need further program refinement, standardization and documentation. The program refinement and standardization includes generalization, for independent SAR data set inputs, addition of a free format control card reader, and internal program documentation. External user oriented program documentation will be generated as input to a SAR/

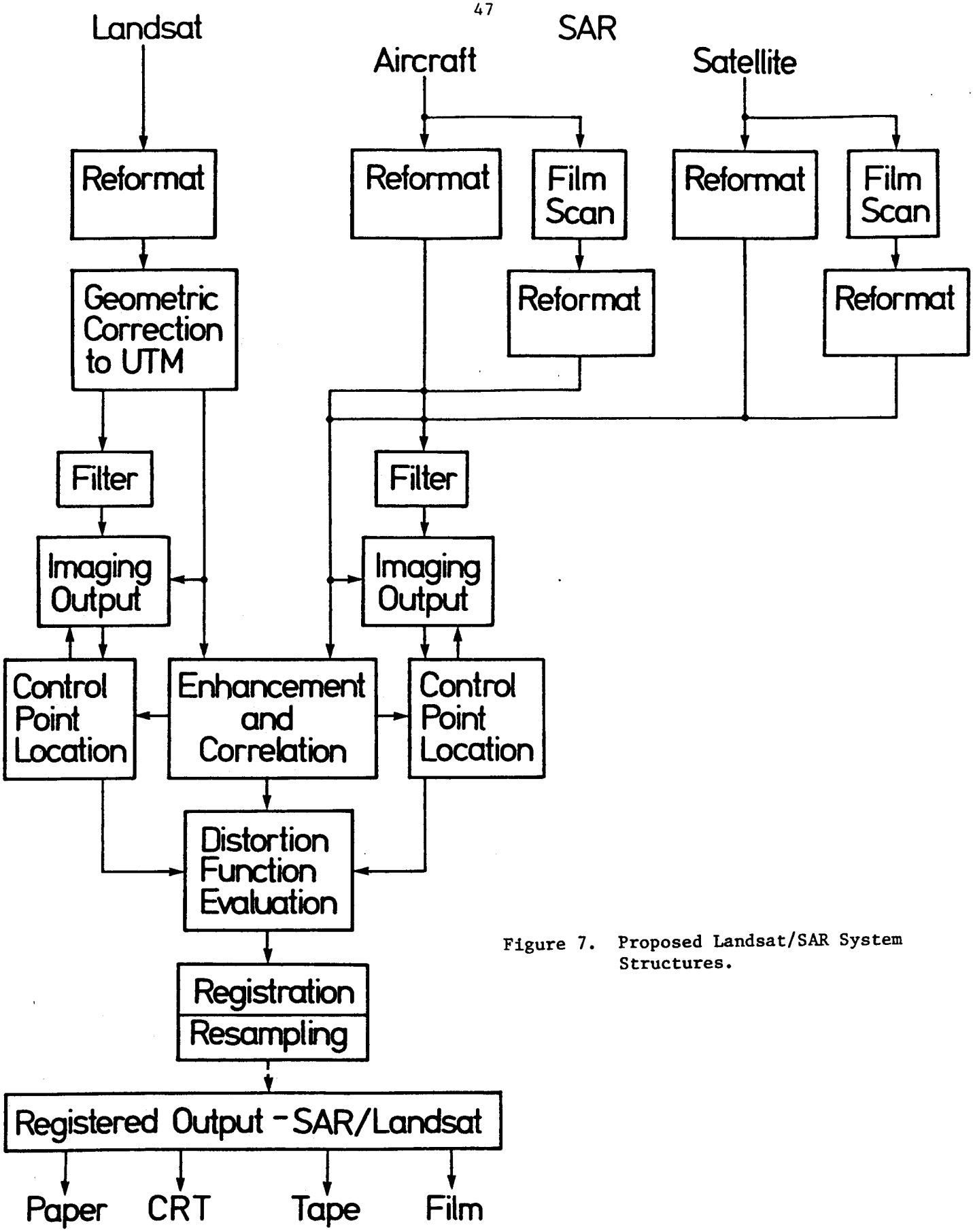

Figure 7. Proposed Landsat/SAR System Structures.

Landsat merging users guide. Phase II will implement SEASAT data reformatting capabilities.

2. Landsat Geometric Correction (Prepared by IBM FSD)

The next level of processing is geometric correction. Landsat data will be processed through IBM software to a UTM grid. Verification of the installation and operation of the software will be a task performed by IBM Federal Systems Division in cooperation with LARS. The Landsat MSS processing software which will be implemented at LARS will be defined in this section. Two options will be defined: Option 1 is a full Landsat MSS processing capability, while Option 2 is a minimal system that satisfies the geometric correction requirement. Option 2 is a subset of Option 1. Each option is described below (See Figure 11).

Option 1 - Full Landsat MSS Processing Capability - The Landsat MSS software will consist of five programs:

- Reformatting Program
- Automatic Control-Point Location Program
- Manual Control-Point Location Program
- Geometric Transformation Program
- Resampling Program

The inputs, functions, and outputs of each of these programs are described below.

There are three kinds of input MSS data that can be processed by the system:

- Uncorrected Data - This consists of bands of MSS data in the X-format. The image data has been radiometrically corrected and line-length adjusted, but no other corrections have been applied. Ancillary data includes no geometric transformation.

- Partially Processed Data - This consists of four or five bands of MSS data in the BSQ format. The only correction applied to the image data is radiometric correction. Ancillary data includes geometric transformation information.
- Fully Corrected Data - This consists of four or five bands of MSS data in the BSQ format. Both radiometric correction and geometric correction have been applied to the data.

The system will be able to geometrically correct and perform a striping reduction on both uncorrected and partially processed data. It will also be able to resample fully corrected data in order to change the pixel spacing.

As shown in Figure 11 there are three paths through the software. The first path involves the reformatting, automatic control-point location, geometric transformation, and resampling programs. This path would normally be used for an uncorrect MSS scene for which a corresponding control-point library exists. The result from this path is a fully corrected MSS scene with user-selected orientation and pixel spacing. This would be the most desirable path for processing uncorrected data. It can also be used to correct partially processed data. If no control-point library exists for an uncorrected MSS scene that is to be processed, there are two alternate paths through the system that can be used.

The second path involves the reformating, geometric transformation, and resampling programs. This path would normally be used for an uncorrected MSS scene for which no control-point library exists or for a partially processed MSS scene. The result from using this path on an uncorrected MSS scene would be a systematically corrected MSS scene with user-selected orientation and pixel spacing. From a partially processed scene, a fully corrected MSS scene that has been either systematically corrected or scene corrected (depending

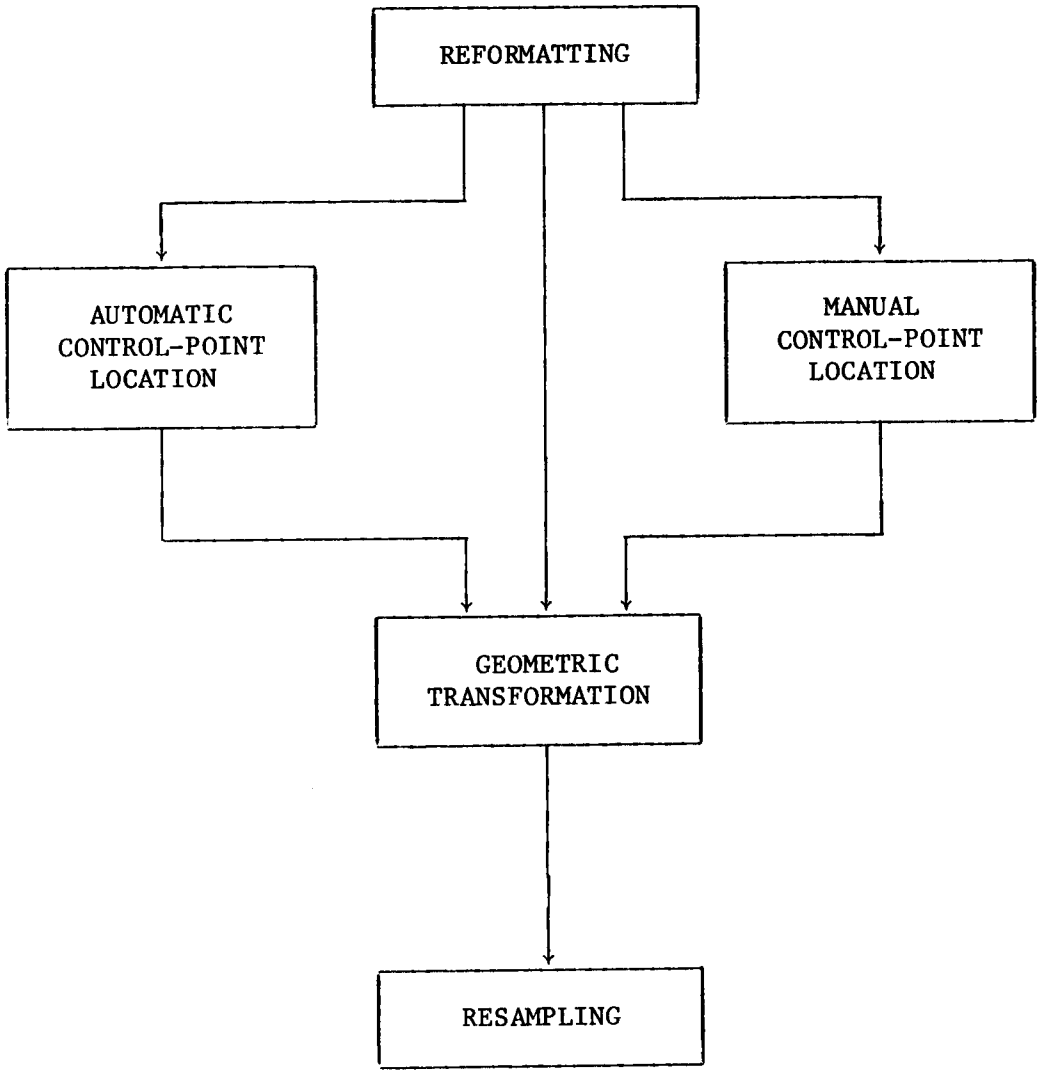

Figure 11. Option 1 Software Paths

on the original ancillary data) can be produced with this path through the software.

The third path involves the reformatting, manual control-point location, geometric correction, and resampling programs. This path would normally be used for an uncorrected MSS scene for which no corresponding control-point library exists or for a fully corrected MSS scene. The result from this path would be a fully corrected MSS scene in either case.

Option 2 - Minimal Landsat MSS Processing Capability - The Landsat MSS software will consist of three programs:

- Reformatting Program
- Geometric Transformation Program
- Resampling Program

The inputs, functions, and outputs of each of these programs are described below.

There are three kinds of input MSS data that can be processed by the system:

- Uncorrected Data - This consists of four bands of MSS data in the X format. The image data has been radiometrically corrected and line-length adjusted, but no other corrections have been applied. Ancillary data includes no geometric transformation.
- Partially Processed Data - This consists of four or five bands of MSS data in the BSQ format. The only correction applied to the image data is radiometric correction. Ancillary data includes geometric transformation information.
- Fully Corrected Data - This consists of four or five bands of MSS data in the BSQ format. Both radiometric correction and geometric correction have been applied to the data.

The merging system will be able to geometrically correct both uncorrected and partially processed data. It will also be able to resample fully corrected data in order to change the pixel spacing. For a fully corrected input scene, only the reformatting and the resampling portion of the manual control-point location program are used. In this case, the result is a fully corrected scene with different pixel spacing.

The grid formed by the corrected Landsat will be used as the reference for all SAR data. Thus, the SAR data will be corrected to this grid during the data merging. Phase II will investigate SEASAT geometric qualities. Phase III would implement results implied from Phase II investigations of SEASAT data.

Film data scanning and digitizing is expected to be a basic part of SAR data handling. Film scanning capability is not provided by the Phase I system implementation; however, this capability is provided by a number of organizations including NASA Wallops. Reformatting capability is included in this task for handling digital data from film scanners. Software will be implemented to provide a basic structure for reformatting any data format.

3. Image Filtering

Filtering of Landsat and SAR data is important to obtain the best possible imaging outputs as well as to bring out full data analysis potentials. Several image filtering methods were evaluated in the previous study and certain of these will be implemented. For SAR processing there are two which appear to be of significant value. One is an along and across data normalization to reduce shading in the SAR imagery. The second is low pass filtering to partially remove speckle due to the nature of the SAR imaging process. Speckle is best reduced at the source by averaging several "looks" taken within the same resolution cell. If however imagery having speckle is on hand and the user

wishes to process it, it may be desirable to spatially filter the data. These capabilities will be implemented. Other filtering operations will be made available in the IBM implementation discussed separately.

4. Imaging

Imaging is one of the most critical functions of the SAR/Landsat data merging system. Currently rudimentary outputs are available from paper, film and digital display. The paper outputs include lineprinter and gray level varian printer/plotter. The lineprinter has low utilization while the gray level printer/plotter output has medium to high utility. The black and white digital display falls in the same category of medium to high utility. The available film recorder has medium utility because of its low resolution and small format. A more versatile color digital display would add measurably to the data merging system. Of high utility to the project would be in-house film scanning and film writing capability. Color film writing is highly desirable. Current external vendor capabilities provide good experimental turnaround, but will not meet the needs of an operational system. High quality imaging is critical to the checkpointing process. Phase II would include procurement of a color digital display and digital film scanner and color film writer. Phase III would refine the implementation of these for better user interaction.

The activities in this task for Phase I will be documentation of procedures for use of the available imaging devices as part of the system document for easy reference by the user.

5. Control Point Location

Control point location will be a manual process with some automated assistance. Current imaging capabilities both in-house and out-of-house will be used fully to provide the quality of image needed to obtain accurate

checkpoint locations. The high resolution film writing outputs have been exceptionally important to successful checkpointing. The electronic table digitizer may be used to measure the locations found for corresponding checkpoints. This process will be further refined and user documented during Phase I. Phase II will be revised slightly for use of new equipment to be procured during this phase. Further investigation will be made into automated cross correlation between SAR and Landsat data.

6. Distortion Evaluation

Image distortion evaluation will be carried out using least squares fit to a number of mathematical models. In the study parametric, affine, quadratic, cubic, fourth and fifth order models were evaluated against the aircraft SAR registration problem. Results indicate the parametric, affine and quadratic representations adequately represented distortions in most cases. It is thus proposed here that these functions plus cubic polynomial representation be implemented in the Phase II system. These functions will enable the user to represent distortion and register most aircraft SAR data sets to a geographic reference. Higher order functions can be implemented later should the need be demonstrated.

The functions to be implemented are for the aircraft SAR case. Correction of Landsat imagery to a cartographic reference will be handled by an IBM system proposed in another section.

Description of distortions in Satellite SAR has not been considered; however, it is expected that the general polynomial representations which will be made available will enable subsets of satellite frames to be registered to a Landsat reference. Further study will be required to define all distortions in Satellite SAR imagery.

The distortion functions proposed for implementation here will be integrated into a user oriented system and documentation generated which will allow a technically trained person to easily utilize the system.

7. Registration and Resampling

Registration is the heart of the SAR Landsat data merging system. Software for this function exists in a highly experimental and inefficient state. During Phase I a new modularly organized registration system is to be written. Internal program documentation will be brought up to a high level as will the user oriented external documentation. Streamlined buffering and location calculation software will assure more economical computer usage. A high degree grid with linear interpolation registration scheme will be implemented. High degree initially will be up to bicubic. Actual data manipulation will be kept to a minimum. During Phase II refinements will be added to include advanced resampling schemes and a higher degree registration if required.

Resampling will be accomplished simultaneously with registration. Resampling schemes to be made available include nearest neighbor and cubic interpolation. These will be written as modularized portions of the registration software. Appropriate internal and user oriented external documentation will be produced. Phase II will include an advanced interpolation scheme yet to be decided.

These elements constitute the system elements to be implemented and documented by LARS. Some include extensive programming and documentation while others consist primarily of documentation. A film scanner/writer and a color video display are needed by the system but are not proposed here. External sources will be utilized for these functions until funding can be obtained for these hardware items.

X. ACKNOWLEDGMENTS

This report contains results of a Landsat/SAR data registration study conducted by LARS. The study as contracted by NASA Wallops involved contributions from LARS, IBM FSD and Goodyear Aerospace Corp. The results from all three organizations are published in a combined system plan document published by NASA. The material in this report represents the LARS contribution; however, some material generated by NASA Wallops and IBM FSD has been included for completeness for readers of this report who may not have the complete NASA report. In particular the material on the systematic correction and Data Set No. 1 analysis was prepared by Dr. Harold Maurer and staff at NASA Wallops. (The comparison in the appendix of the systematic and affine method was done at LARS by Timothy Grogan.) The description of the Landsat correction system was prepared by Steven Murphry and others at IBM FSD. No material by Goodyear Aerospace has been included; however, their tutorial help was significant in aiding the LARS work. It is hoped that this document will be generally useful as well as satisfying the final report requirements of the contract.

XI. BIBLIOGRAPHY

"Study of Synthetic Aperture Radar (SAR) Imagery Characteristics," Goodyear Aerospace Corp. Report GERA-2089, May 30, 1975.

Chafaris, G. J., "Definition of the Major Applications and Requirements Relative to Overlaying SEASAT-A SAR and Landsat MSS Data Sets," Final Report for NASA Contract NAS5-23412 Ammendment 126, June 8, 1978, General Electric Co., Beltsville, Md.

Tomiyasu, Kiyo, "Tutorial Review of Synthetic-Aperture Radar (SAR) with Applications to Imaging of the Ocean Surface," Proc. of IEEE, Vol. 66, No. 5, May 1978, pp. 563-583.

"Synthetic Aperture Radar/Landsat Image Registration System Plan," NASA Contractor Report.

Jordan, R. L., Rodgers, D. H., "A SEASAT-A Synthetic Aperture Imaging Radar System" Conference Proceedings Paper, source not available, JPL, Pasadena, Calif.

Bayma, R. W., Jordan, R. I., Manning, B. N., "A Survey of SAR Image-Formation Processing for Earth Resources Applications," Proceedings of 11th Intl. Symposium on Remote Sensing of Environment, 25-29 April 1977, Ann Arbor, Mich.

APPENDIX

Comparison of LARS Affine and Wallops Systematic Error Model

The systematic error model and LARS Affine programs model geometric distortion in an image with respect to a reference image. The programs model rotation angle, range scale, track scale, and shear angle distortions. An outline of the systematic error model program operation is described in the NASA/WALLOPS SYNTHETIC APERTURE RADAR IMAGE PROCESSING, SYSTEM PLAN. So it will not be repeated here. A flowchart of the program operation and of the program mathematics are provided in Figure 12 and 13, respectively.

The systematic error model program can be shown to be essentially the same six parameter affine model used in the LARS AFFINE program. The following shows that the systematic error program is a six parameter affine model.

Let, $P \triangleq$ map track control point coordinates
$Q \triangleq$ map range control point coorindates
$X \triangleq$ distorted track control point coordinates
$Y \triangleq$ distorted range control point coordinates
$P' \triangleq$ rotated track control point coordinates
$Q' \triangleq$ rotated range control point coordinates

The mathematical description of the program provides the model:

$$P_i' = A_6(X_i + K(0.00005)Y_i) + \left(\sum_{j=1}^{N} (B_6 + r_{6j}^{x}) \right)/N$$

$$Q_i' = A_3 Y_i + \left(\sum_{j=1}^{N} (B_3 + r_{3j}^{Y}) \right)/N \quad ,$$

where $\sum_{j=1}^{N} (r_{6i}^{x})^2$ is a minimum and where $K \epsilon I$ such that $\sum_{i=1}^{N} |r_{6i}^{x}|$ is a minimum; also $\sum_{i=1}^{N} (r_{3i}^{y})^2$ is a minimum.

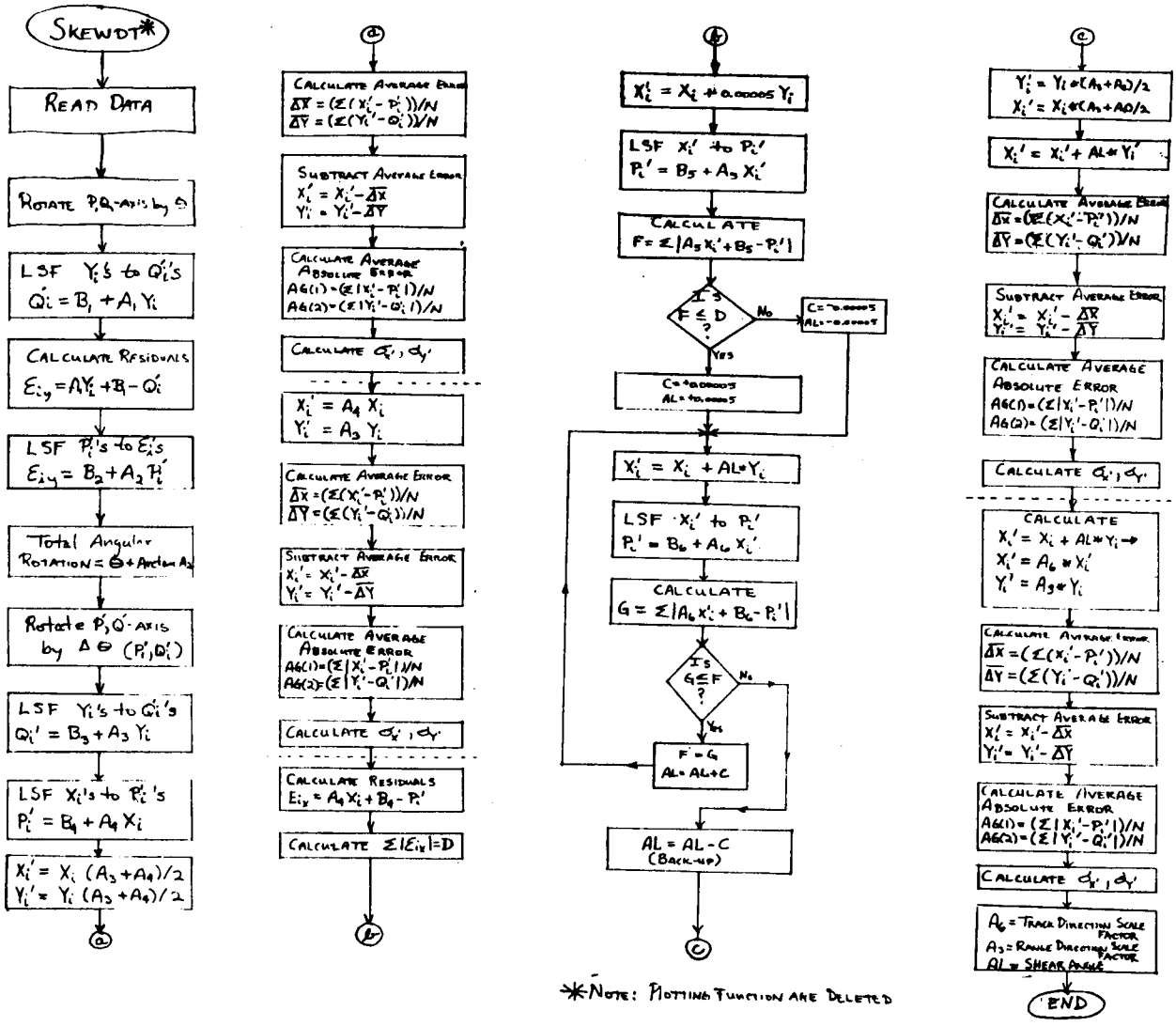

Figure 9. Flow chart for NASA/Wallops Systematic Error Program (i.e., Subroutine SKEWDT)

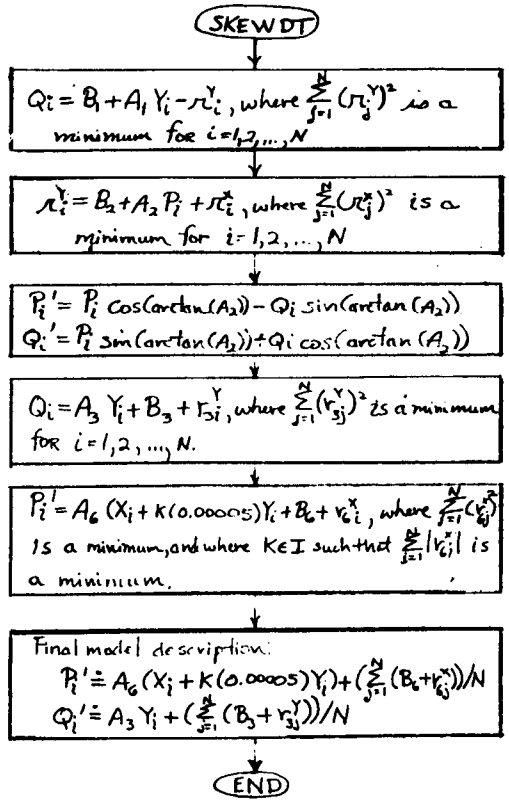

Mathematical description of Systematic error model program

Figure 10 Mathematical Model for Systematic Error Program

This is a least-square approximation. First, in least-squares $\sum_{i=1}^{N} r_i = 0$. So, the calculation of $\overline{\Delta(\cdot)} = B_{(\cdot)}$. The calculation of $\overline{\Delta x}$ and $\overline{\Delta Y}$ in the program is redundent in those cases where the scale and not the average scale is used in modeling. With this simplification and allowing AL = K(0.00005), the model becomes

$$P_i' \cong A_6(X_i + AL\ Y_i) + B_6$$

$$Q_i' \cong A_3\ Y_i + B_3$$

where the approximation is in the least squares sense. Introducing now the model of the rotation

$$P_i' = P_i*\cos(ARAD) - Q_i*\sin(ARAD) = A_6*(X_i + AL*Y_i) + B_6$$

$$Q_i' = P_i*\sin(ARAD) + Q_i*\cos(ARAD) = A_3*Y_i + B_3$$

where ARAD = angle of rotation; A_6 = track scale factor; AL = shear; A_3 = range scale factor; B_6 = translation in track; B_3 = translation in range

Since ARAD is obtained by a least-squares approximation, the coordinates rotated and least-squares again applied, the model is overall a least-squares approximation.

Solving the above equations for P_i and Q_i,

$$P_i = A_6*\cos(ARAD)*X_i+(A_3*\sin(ARAD)+A_6*AL*\cos(ARAD)*Y_i + B_6*\cos(ARAD)+B_3*\sin(ARAD)$$

$$Q_i=(-A_6*\sin(ARAD))*X_i+(-A_6*AL*\sin(ARAD)+A_3*\cos(ARAD))*Y_i -B_6*\sin(ARAD)+B_3*\cos(ARAD)$$

or more simply

$$P_i = AF*X_i+BF*Y_i+CF$$

$$Q_i = DF*X_i+EF*Y_i+FF \quad ,$$

which is a six parameter affine transformation.

The LARS AFFINE program performs a six parameter least-squares fit for the delta functions

$$\Delta_x(X^A,Y^A) = X^B - X^A = a_o + a_1 * X_i^A + a_2 * Y_i^A$$

$$\Delta_y(X^A,Y^A) = Y^B - Y^A = b_o + b_1 * X_i^A + b_2 * Y_i^A ,$$

where superscripts A and B denote RUNA image and RUNB image, respectively. When the transformation is implemented, for each point in the area in the RUNA image to be registered the delta functions are computed. This transform the RUNA image coordinate (LANDSAT) to the RUNB to the RUNB image coordinates (SAR). This determines the pixel (or interpolated pixel set) in the RUNB image to overlay at the corresponding RUNA coordinate position. This is the inverse operation of the systematic error model, if the P,Q(map coordinates) are regarded as the LANDSAT and the distorted image (X,Y coordinates), the SAR. Therefore, when residual errors were quoted in the Affine program, the errors are with respect to the RUNB or SAR image. When residual errors were quoted in the systematic error model program the errors are with respect to the X,Y or LANDSAT image. The resolution in the SAR image is usually much finer than that of the LANDSAT. So an error of 1 pixel in the LANDSAT image and quoted by the systematic error model program might map into an error of 3 pixels in the SAR image and so stated by the Affine program. This is due to the scaling differences between the images. The circular error in each reference frame are related by $(S_x\sigma_{xA})^2 + (S_y\sigma_{yA})^2 = (\sigma_{xB}^2+\sigma_{yB}^2)$.

The following shows that if the checkpoint pairs are reversed in the systematic error model program, then the LARS Affine and the systematic error model program are identical.

The systematic program model has been shown to be

$$P_i = AF * X_i + BF * Y_i + CF$$

$$Q_i = EF * X_i + CF * Y_i + FF$$

If the P,Q coordinate pair is allowed to represent the RUNB coordinates and X,Y coordinates the RUNA coordinates, then

$$X^B = AF*X^A+BF*Y^A+CF$$

$$Y^B = DF*X^A+EF*Y^A+FF \quad .$$

The model used for the LARS Affine program is

$$\Delta_x(X^A,Y^A) = X^B-X^A = a_o+a_1*X^A+a_2*Y^A$$

$$\Delta_y(X^A,Y^A) = Y^B-Y^A = b_o+b_1*X^A+b_2*Y^A \quad .$$

So,
$$X^B = a_o+(a_1+1)*X^A+a_2*Y^A$$

$$Y^B = b_o+b_1*X^A+(b_2+1)*Y^A \quad .$$

Therefore, the models are equivalent where

$$a_o = CF \qquad a_1 = AF-1 \qquad a_2 = BF$$

$$b_o = FF \qquad b_1 = DF \qquad b_2 = EF-1 \quad .$$

The program for the systematic error model was edited so that the reversal was obtained. A subroutine, AFFPAR, was amended to the systematic program to calculate the affine and LARS "delta" Affine parameters. Another subroutine, RESID, was also added to the systematic program to calculate residual errors between the initial map coordinates and rotated coordinates using the model.

An example showing the equivalence of the two programs and an example showing corresponding changes in the r.m.s. error when the mapping is reversed are shown in Figures 14 and 15. Here it should be noted that the "Variance" shown in the WALLOPS program description outline and in the labeling of the printed results is actually the standard deviation not the variance.

SKEW DETERMINATION

P(LINE)	Q(COL)	X(LINE)	Y(COL)
305.	701.	818.	917.
482.	406.	885.	918.
491.	780.	821.	963.
435.	636.	842.	935.
402.	544.	855.	917.
719.	509.	888.	978.
668.	688.	852.	988.
667.	845.	824.	1006.
820.	560.	888.	1005.
568.	1030.	783.	1004.
922.	610.	888.	1031.
919.	852.	845.	1058.
821.	318.	930.	978.
205.	840.	785.	910.
397.	871.	796.	952.
628.	207.	930.	926.
670.	1083.	783.	1032.
827.	69.	972.	951.

ANGULAR ROTATION = 113.2649 DEGREES

ERROR AFTER ROTATION, SCALE , TRANSLATION, & SHEAR

TABLE I - RESIDUAL ERRORS

POINT NUMBER	T ACK ERROR	RANGE ERROR
1	1.51	0.54
2	-0.00	-0.67
3	0.91	-0.10
4	0.97	-1.19
5	0.13	-1.55
6	0.10	-0.66
7	0.08	-0.01
8	0.26	0.92
9	0.70	-0.36
10	-2.32	0.20
11	0.19	-0.25
12	0.16	0.74
13	0.77	-0.43
14	-0.66	-0.16
15	-1.42	0.03
16	-0.27	1.58
17	-1.09	0.49
18	-0.01	0.91

AVERAGE ERROR MAGNITUDE
X = 0.6410
Y = 0.6005
X VARIANCE = 0.8930Y VARIANCE = 0.7615

THE TRACK DIRECTION SCALE FACTOR IS 1# -0.2219 , THE RANGE DIRECTION SCALE FACTOR IS 1# -0.2032, THE SHEAR IS -4.084 DEGREES

********** LARS RESID CALCULATION OF RESIDUALS **********

RUNA LINE	RUNA COLUMN	RUNB LINE	RUNB COLUMN	COMPUTED LINE	COMPUTED COLUMN	LINE ERROR	COLUMN ERROR
305.	701.	818.	917.	817.90	915.40	0.104	1.600
482.	406.	885.	918.	884.38	918.27	0.620	-0.268
491.	780.	821.	963.	820.55	962.81	0.454	0.192
435.	636.	842.	935.	840.52	934.54	1.480	0.458
402.	544.	855.	917.	853.52	917.50	1.476	-0.498
719.	509.	888.	978.	887.35	978.17	0.646	-0.174
668.	688.	852.	988.	851.96	987.93	0.045	0.069
667.	845.	824.	1006.	824.74	1005.40	-0.740	0.598
820.	560.	888.	1005.	887.39	1004.50	0.607	0.496
568.	1030.	783.	1004.	784.10	1006.05	-1.098	-2.049
922.	610.	888.	1031.	887.69	1030.92	0.307	0.076
919.	852.	845.	1058.	845.62	1057.56	-0.615	0.442
821.	318.	930.	978.	929.30	977.46	0.705	0.537
205.	840.	785.	910.	785.11	910.67	-0.114	-0.665
397.	871.	796.	952.	796.58	953.29	-0.585	-1.292
628.	207.	930.	926.	931.56	925.63	-1.560	0.375
670.	1083.	783.	1032.	783.88	1032.81	-0.879	-0.808
827.	69.	972.	951.	972.85	950.65	-0.845	0.347

	LINE	COLUMN
AVERAGE ERROR	0.00	-0.00
ABSOLUTE AVG. ERROR	0.72	0.64
R.M.S. ERROR	0.842	0.818

AFFINE PARAMETERS
X1= 0.887639 *X + -0.172787 *Y + 912.289716
Y1= 0.203840 *X + 0.112581 *Y + 774.309689

AFFINE DELTA PARAMETERS
DELTA X= -0.912361 *XA + -0.172787 *YA + 912.289716
DELTA Y= 0.203840 *XA + -0.887419 *YA + 774.309689

Figure 11. Systematic Error Model Program Example Results with Checkpoint Pairs Reversed.

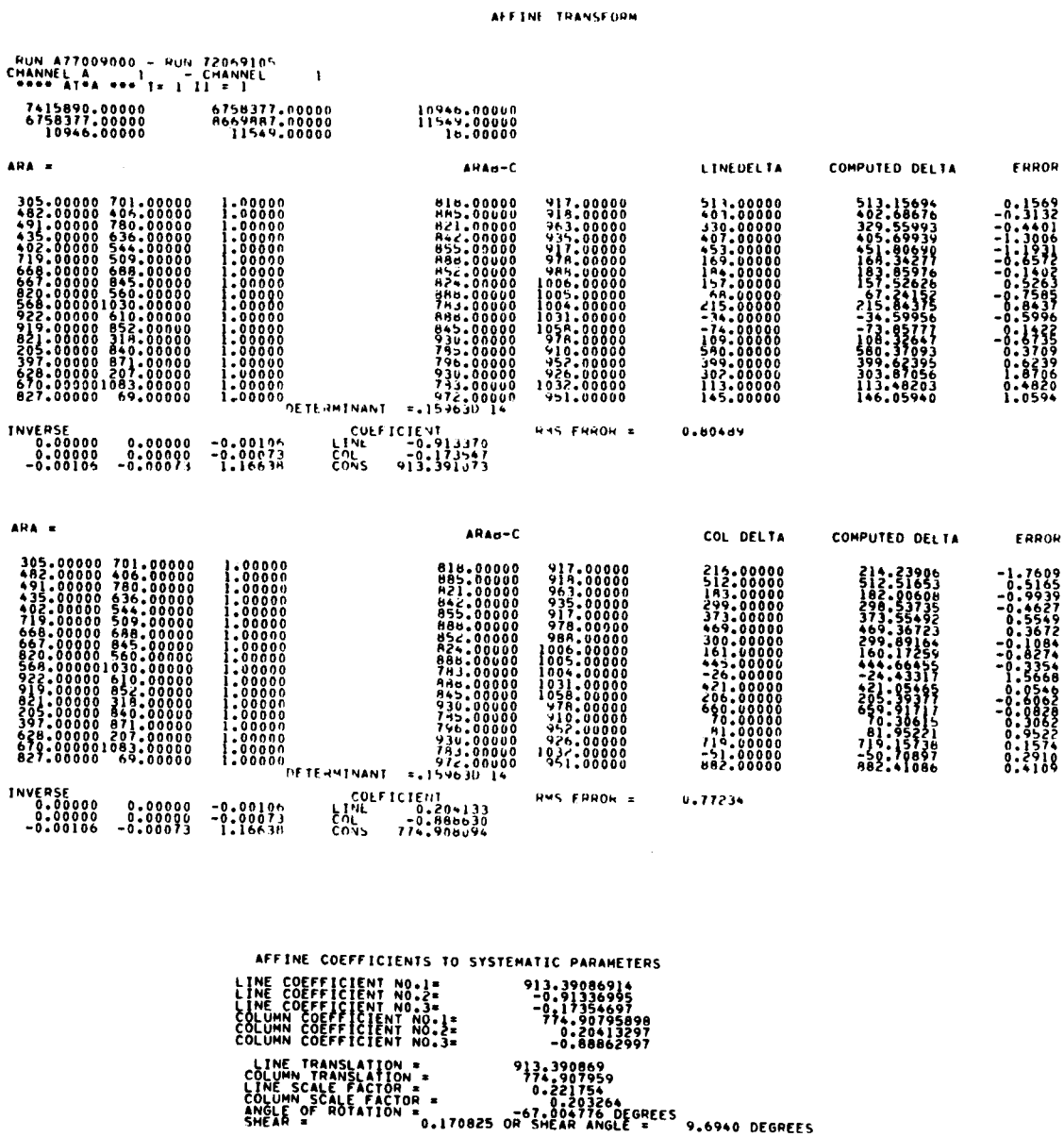

```
                                        AFFINE TRANSFORM

 RUN A77009000 - RUN 72069105
CHANNEL A      1    - CHANNEL      1
 **** AT*A *** I= 1 II = 1

   7415890.00000        6758377.00000          10946.00000
   6758377.00000        8669887.00000          11549.00000
     10946.00000          11549.00000             18.00000

ARA =                                    ARAB-C                    LINEDELTA      COMPUTED DELTA      ERROR

 305.00000 701.00000   1.00000          818.00000   917.00000      513.00000      513.15694          0.1569
 482.00000 406.00000   1.00000          885.00000   918.00000      401.00000      402.68676         -0.3132
 491.00000 780.00000   1.00000          821.00000   963.00000      330.00000      329.55993         -0.4401
 435.00000 636.00000   1.00000          842.00000   935.00000      407.00000      405.69939         -1.3006
 402.00000 544.00000   1.00000          855.00000   917.00000      453.00000      451.80690         -1.1931
 719.00000 509.00000   1.00000          888.00000   978.00000      169.00000      169.34277          0.6577
 668.00000 688.00000   1.00000          852.00000   984.00000      194.00000      193.85976         -0.1402
 667.00000 845.00000   1.00000          824.00000  1006.00000      157.00000      157.52626          0.5263
 820.00000 560.00000   1.00000          888.00000  1005.00000       68.00000       67.24152         -0.7585
 568.00000 1030.00000  1.00000          783.00000  1004.00000      215.00000      215.84375          0.8437
 922.00000 610.00000   1.00000          888.00000  1031.00000      -34.00000      -34.59956         -0.5996
 919.00000 852.00000   1.00000          845.00000  1058.00000      -74.00000      -73.85777          0.1422
 821.00000 318.00000   1.00000          930.00000   978.00000      109.00000      108.32647         -0.6735
 205.00000 840.00000   1.00000          745.00000   910.00000      580.00000      580.37093          0.3709
 397.00000 871.00000   1.00000          796.00000   957.00000      399.00000      399.62395          0.6239
 628.00000 207.00000   1.00000          930.00000   926.00000      302.00000      303.87056          1.8706
 670.00000 1083.00000  1.00000          783.00000  1032.00000      113.00000      113.48203          0.4820
 827.00000  69.00000   1.00000          972.00000   951.00000      145.00000      146.05940          1.0594
                              DETERMINANT =.159630 14

INVERSE                                  COEFICIENT                RMS ERROR =    0.80489
   0.00000   0.00000  -0.00106   LINE     -0.913370
   0.00000   0.00000  -0.00073   COL      -0.173547
  -0.00106  -0.00073   1.16638   CONS    913.391073

ARA =                                    ARAB-C                    COL DELTA      COMPUTED DELTA      ERROR

 305.00000 701.00000   1.00000          818.00000   917.00000      216.00000      214.23906         -1.7609
 482.00000 406.00000   1.00000          885.00000   918.00000      512.00000      512.51653          0.5165
 491.00000 780.00000   1.00000          821.00000   963.00000      183.00000      182.00608         -0.9939
 435.00000 636.00000   1.00000          842.00000   935.00000      299.00000      298.53735         -0.4627
 402.00000 544.00000   1.00000          855.00000   917.00000      373.00000      373.55492          0.5549
 719.00000 509.00000   1.00000          888.00000   978.00000      469.00000      469.36723          0.3672
 668.00000 688.00000   1.00000          852.00000   984.00000      300.00000      299.89164         -0.1084
 667.00000 845.00000   1.00000          824.00000  1006.00000      161.00000      160.17259         -0.8274
 820.00000 560.00000   1.00000          888.00000  1005.00000      445.00000      444.66455         -0.3354
 568.00000 1030.00000  1.00000          783.00000  1004.00000      -26.00000      -24.43317          1.5668
 922.00000 610.00000   1.00000          888.00000  1031.00000      421.00000      421.05465          0.0546
 919.00000 852.00000   1.00000          845.00000  1058.00000      206.00000      205.39377         -0.6062
 821.00000 318.00000   1.00000          930.00000   978.00000      660.00000      659.91717         -0.0828
 205.00000 840.00000   1.00000          745.00000   910.00000       70.00000       70.30615          0.3062
 397.00000 871.00000   1.00000          796.00000   957.00000       81.00000       81.95221          0.9522
 628.00000 207.00000   1.00000          930.00000   926.00000      719.00000      719.15738          0.1574
 670.00000 1083.00000  1.00000          783.00000  1032.00000      -51.00000      -50.70897          0.2910
 827.00000  69.00000   1.00000          972.00000   951.00000      882.00000      882.41086          0.4109
                              DETERMINANT =.159630 14

INVERSE                                  COEFICIENT                RMS ERROR =    0.77234
   0.00000   0.00000  -0.00106   LINE      0.204133
   0.00000   0.00000  -0.00073   COL      -0.888630
  -0.00106  -0.00073   1.16638   CONS    774.908094

        AFFINE COEFFICIENTS TO SYSTEMATIC PARAMETERS

LINE COEFFICIENT NO.1=          913.39086914
LINE COEFFICIENT NO.2=           -0.91336995
LINE COEFFICIENT NO.3=           -0.17354697
COLUMN COEFFICIENT NO.1=        774.90795898
COLUMN COEFFICIENT NO.2=          0.20413297
COLUMN COEFFICIENT NO.3=         -0.88862997

 LINE TRANSLATION =            913.390869
COLUMN TRANSLATION =           774.907959
LINE SCALE FACTOR =              0.221754
COLUMN SCALE FACTOR =            0.203264
ANGLE OF ROTATION =          -67.004776 DEGREES
SHEAR =          0.170825 OR SHEAR ANGLE =     9.6940 DEGREES
```

Figure 12. LARS AFFINE Model Program Example Results with Checkpoint Pairs Reversed.

By comparing the results of the two programs, they are essentially the same model (allowing for small computational errors). The differences noticed between the r.m.s. errors calculated by the systematic program and by RESID are due to the fact that errors computed in the program are with P&Q rotated with respect to X&Y. In RESID errors are computed with X,Y rotated with respect to P&Q. Therefore, a small error is interchanged between the line and column errors between the two calculations.

The LARS Affine program obtains the model in total with only one least-squares fit, while the systematic program requires at least six to obtain the same result. The additional insight the systematic error program provides in printing rotation angle, scaling, and shear angle can be obtained in the LARS program with the addition of a simple subroutine calculation. The following is a derivation of the necessary subroutine calculations.

$$\begin{bmatrix} X^B \\ Y^B \end{bmatrix} = \underbrace{\begin{bmatrix} +\cos\theta & +\sin\theta \\ -\sin\theta & +\cos\theta \end{bmatrix}}_{\text{rotation}} \underbrace{\begin{bmatrix} 1 & \alpha \\ 0 & 1 \end{bmatrix}}_{\text{Shear}} \underbrace{\begin{bmatrix} S_x & 0 \\ 0 & S_y \end{bmatrix}}_{\text{Scale}} \begin{bmatrix} X^A \\ Y^A \end{bmatrix} + \underbrace{\begin{bmatrix} a_o \\ b_o \end{bmatrix}}_{\text{Translation}}$$

$$\begin{bmatrix} X^B \\ Y^B \end{bmatrix} - \begin{bmatrix} X_x\cos\theta & \alpha S_y\cos\theta - s_y\sin\theta \\ -S_x\sin\theta(-\alpha S_y\sin\theta)+S_y\cos\theta & \end{bmatrix} \begin{bmatrix} X^A \\ Y^A \end{bmatrix} + \begin{bmatrix} a_o \\ b_o \end{bmatrix}$$

The AFFINE delta function

$$\begin{bmatrix} X^B \\ Y^B \end{bmatrix} - \begin{bmatrix} X^A \\ Y^A \end{bmatrix} = \begin{bmatrix} a_1 \\ b_1 \end{bmatrix} \begin{bmatrix} a_2 \\ b_2 \end{bmatrix} \begin{bmatrix} X^A \\ Y^A \end{bmatrix} + \begin{bmatrix} a_o \\ b_o \end{bmatrix}$$

or

$$\begin{bmatrix} X^B \\ Y^B \end{bmatrix} = \begin{bmatrix} a_1+1 & a_2 \\ b_1 & b_2+1 \end{bmatrix} \begin{bmatrix} X^A \\ Y^A \end{bmatrix} + \begin{bmatrix} a_o \\ b_o \end{bmatrix}$$

Solving these for θ, S_y, S_x, and α,

$$\theta = \arctan\left(\frac{-b_1}{a_1+1}\right) \qquad S_x = \frac{a_1+1}{\cos\theta}$$

$$S_y = (b_2+1)\cos\theta + a_2\sin\theta \qquad \alpha = \frac{[a_2\cos\theta] - [(b_2+1)\sin\theta]}{S_y}$$

In implementing these relations the single least-squares fit operation of the LARS Affine program will also provide a parametric description of the distortion. Table 7 provides comparison of the systematic error model and the LARS affine model. The direction of the scaling and the angular rotations apparently differ. They are actually the same. The LARS affine calculation of the parameter chooses the rotation and scale directions such that the line scale factor is always positive. The small errors between the LARS affine and systematic calculated residuals are a result of the systematic error model which rotates the reference and then scales and srews, where the LARS model rotates the distorted image.

Table 7. Comparison of WALLOPS Systematic Error Model and LARS Affine Model.

	FORWARD		REVERSED	
	LARS AFFINE	WALLOPS SYSTEMATIC	LARS AFFINE	WALLOPS SYSTEMATIC
LINE RMS ERROR	3.82530	4.1923 (3.829)*	0.80489	0.8930 (0.842)*
COLUMN RMS ERROR	3.63939	3.1940 (3.622)*	0.77234	0.7615 (0.818)*
LINE TRANSLATION	-5238.323913	-5242.444701	913.391073	912.289716
COLUMN TRANSLATION	2646.570270	2653.129237	774.8094	774.309689
TRACK SCALE	5.157719	-5.1582	0.221754	-0.2219
RANGE SCALE	4.299145	-4.2992	0.203264	-0.2032
ROTATION ANGLE	61.387711°	-118.6180°	-67.004776°	113.2649°
SHEAR ANGLE	2.0788°	-1.822°	9.6940°	-9.084°

*LARS calculation of residual in systematic error program